

# Understanding the Engines and Progenitors of Gamma-Ray Bursts

Chris L. Fryer<sup>1,2</sup>, Nicole Lloyd-Ronning<sup>1,3</sup>, Ryan Wollaeger<sup>1</sup>, Brandon Wiggins<sup>1,4</sup>, Jonah Miller<sup>1,5</sup>, Josh Dolence<sup>1</sup>, Ben Ryan<sup>1</sup>, Carl E. Fields<sup>1,6</sup>

<sup>1</sup> Center for Theoretical Astrophysics, Los Alamos National Laboratory, Los Alamos, NM 87544

<sup>2</sup> Department of Physics, The George Washington University, Washington, DC 20052

<sup>3</sup> University of New Mexico, Los Alamos, NM 87544

<sup>4</sup> Department of Physical Science, Southern Utah University, Cedar City, Utah 84721

<sup>5</sup> Center for Nonlinear Studies, Los Alamos National Laboratory, Los Alamos, NM, USA

<sup>6</sup> Department of Physics and Astronomy, Michigan State University, East Lansing, MI 48824

Received: date / Revised version: date

**Abstract.** Our understanding of the engines and progenitors of gamma-ray bursts has expanded through the ages as a broader set of diagnostics has allowed us to test our understanding of these objects. Here we review the history of the growth in our understanding, focusing on 3 leading engines and 9 potential progenitors. The first gravitational wave detection of a short burst is the latest in a series of breakthrough observations shaping this understanding and we study the importance of multi-diagnostic, multi-messenger observations on these engines and their progenitors. Our understanding based on a detailed study of nearby bursts can be applied to make predictions for the trends expected as we begin to observe high redshift bursts and we discuss these trends.

**PACS.** 95.85.Pw gamma-ray – 95.85.Sz gravitational radiation, magnetic fields, and other observations

## 1 Introduction

50 years ago, the Vela satellites observed the first in a series of bursts of gamma-ray emission. The first 16 bursts were published in a compilation in 1973 [Klebesadel et al., 1973]. The road to understanding the nature (energies, populations, engines, progenitors, environments, etc.) of these gamma-ray bursts (GRBs) has sometimes wandered, but a broad range of diagnostic signposts have led to a continual refinement of GRB models. In this paper, we review this 50 year journey in understanding the origin of, and engines behind, these powerful cosmic explosions. Observations have whittled down the hundreds of models arising from the creative minds of theorists to a few classes of models. These varied and multi-messenger constraints have shaped our understanding of the origin of these bursts. The detection of gravitational waves associated with a gamma-ray burst is just one (albeit a very important one) in a long history of diagnostics used in this study. The many diagnostics (using a broad range of photon energies probing different aspects of the explosions as well as gravitational waves) have helped, and continue to help, astrophysicists probe the details of the engines and progenitors of these bursts, in addition to studying the fundamental physics behind these engines. In this paper, we review the wide range of diagnostics that have shaped our understanding of the short-duration

GRB (sGRB) engine. We study these diagnostics over the broad 50 year journey, beginning with the observational constraints from the first 3 decades (Section 2) and the models (Section 3) and progenitors (Section 4) favored by these observations. The distribution of durations (Section 5) allowed astrophysicists to distinguish between progenitor models and more detailed calculations led to a set of observational predictions (Section 6). Observations confirming some of these predictions have led to the emergence of a favored engine behind GRBs. But, as we have seen with GW170817, the iterations between theory and observation have only just begun with better data making more detailed theory necessary. We conclude with a description of future prospects with GRB observations.

## 2 Observations and Models in the first 3 decades

With the discovery of GRBs, astrophysicists began to design missions focused on finding more. The Burst And Transient Source Experiment (BATSE) [Fishman et al., 1993] produced a large database of gamma-ray bursts, allowing astrophysicists to discern different GRB subgroups: short, hard bursts and long, soft bursts [Mazets et al., 1983, Kouveliotou et al., 1993]. The short bursts had durations from a few milliseconds to a few seconds. The

long bursts were typically a few seconds to a few hundred seconds in duration although classes of very and ultra-long bursts exist with timescales exceeding 1000 s [Levan et al., 2014]. There were spectral differences as well: short bursts typically had higher hardness ratios (more flux in higher energy bands) than the long bursts. In both cases, the gamma-ray emission is highly variable with variability timescales below 1 s.

Models for these bursts ranged from nearby events (lightning storms in the upper Earth’s atmosphere) to very distant explosions (cosmic string interactions in the early universe) [Nemiroff, 1994]. Initially, all models were possible. But the growing observational sample began to constrain these proposed models. For example, although the gamma-ray observations did not exactly pinpoint the burst location, astrophysicists were able to statistically study their distribution, finding that these bursts were isotropically distributed [Briggs, 1993]. Most Earth atmosphere or Galactic models struggled to reproduce these observations. Without a probe beyond the gamma-rays, these arguments were limited; e.g., astrophysicists could test distances by imposing specific theoretical models to make predictions on the distributions. This changed when the accurate localization of GRB970228 by the Italian-Dutch BeppoSAX satellite led to the discovery of its X-ray and optical afterglow and subsequent association with a host galaxy [Costa et al., 1997, van Paradijs et al., 1997]. By assuming the association of the burst with a host galaxy was not coincidence, astrophysicists could pin down the distance of the burst. GRB970508 brought even more conclusive evidence that these bursts must be extragalactic. In the follow-up optical measurements of this burst, astrophysicists observed absorption lines indicating a redshift of at least 0.835 [Metzger et al., 1997]. Radio scintillation measurements that, coupled with the assumption of a nearly speed of light expansion, confirmed the spectral redshift measurement [Frail et al., 1997]. After these two bursts, there was no doubt that some bursts were extragalactic and, with these large distances, astrophysicists could place energy constraints on the bursts and these high energies,  $\sim 10^{51}$  erg (after corrected for beaming), required catastrophic events. Let us review the diagnostics in the first 30 years:

- The gamma-rays from GRBs are variable on the millisecond timescale
- The duration of the gamma-ray emission ranges from a few milliseconds to few hundred seconds
- Two (at least two) classes of bursts exist (short, hard and long, soft) and it may be that multiple models are required to match the data
- Bursts require supernova-like energetics ( $10^{51}$  erg)
- The broadband spectra appear to be power-laws without features and a peak near an MeV.

These constraints, obtained by diagnostics that spanned a range of wavelengths and probed different aspects of the explosion, were sufficient to drive the development of the current “standard” GRB models. In the next few sections, we review these models and discuss how the multi-probe diagnostics were used to focus on the GRB engine.

### 3 Engines and Energetics

The rapid variability of GRBs suggests extreme conditions where the emission environment changes on millisecond timescales. For the powerful engines needed to explain extragalactic sources, the options for rapid variability quickly narrows down to only a few possibilities. Engines active just above the surface of a neutron star (NS) or black hole (BH) soon became favored. The timescale for variabilities in the accretion disk on a NS or BH or instabilities in the magnetic field structure or spin down in a rapidly rotating NS will be on order of this sound crossing or orbital time, e.g.:

$$t_{\text{variability}} \approx R_{\text{NS}}/c_s \approx 0.1\text{ms} \quad (1)$$

where  $R_{\text{NS}} \approx 10^6$  cm and  $c_s \approx 10^{10}$  cm s $^{-1}$ . The potential to produce  $10^{51}$  erg bursts coupled to the ability to have rapid variability led astrophysicists to focus on these NS and BH engines. The difficulty then became determining how to drive an engine on these compact objects. A number of power sources have been suggested, for example:

- Neutron Star Phase Transition: Burst powered by the potential energy release when a phase transition to quark matter occurs in a neutron star [Ramaty et al., 1980, Ma and Xie, 1996]
- Magnetar: Burst powered by a rapidly spinning neutron star with strong magnetic fields [Duncan and Thompson, 1996]
- Neutron star accretion disk (NSAD): Burst powered by accretion onto a neutron star
- Black hole accretion disk (BHAD): Burst powered by accretion onto a black hole [Narayan et al., 1992, Woosley, 1993]

This is far from a complete list, but it gives a flavor of these compact remnant models. Simulations of phase transitions have not produced the high Lorentz factors needed, e.g., see Fryer and Woosley [1998a]. We will thus consider only the latter 3 models, first studying the magnetar engine. With strong (magnetar-strength:  $\sim 10^{15}$  Gauss) magnetic fields, a pulsar can quickly release the rotational energy of a newly formed neutron star. To calculate the energy available for such a model, we need to estimate the rotational energy of the neutron star. The moment of inertia of neutron stars depends upon the equation of state [Worley et al., 2008], but all estimates of the moment for a neutron star ( $I_{\text{NS}}$ ) are within a factor of two of:

$$I_{\text{NS}} = 10^{45} (M_{\text{NS}}/M_{\odot}) g \text{ cm}^2 \quad (2)$$

where  $M_{\text{NS}}$  is the neutron star mass. The corresponding rotational energy ( $E_{\text{rot}}$ ) is:

$$E_{\text{rot}} = 1/2 I_{\text{NS}} \omega^2 = 5 \times 10^{50} (\omega/1000 \text{ Hz})^2 \text{ erg} \quad (3)$$

where  $\omega$  is the angular velocity. If the neutron star is spinning with a ms period, it can produce a  $10^{51}$  erg explosion if it can tap 10% of the rotational energy to drive a jet.

The energy released in an accreting neutron star or black hole is set by the potential energy released by the accreting matter ( $E_{\text{acc}}$ ):

$$E_{\text{acc}} = GM_{\text{NS,BH}}m_{\text{acc}}/R_{\text{NS,BH}} - GM_{\text{NS,BH}}m_{\text{acc}}/R_0 \quad (4)$$

where  $G$  is the gravitational constant,  $M_{\text{NS,BH}}$  is the neutron star or black hole mass,  $m_{\text{acc}}$  is the accreted mass,  $R_{\text{NS,BH}}$  is the neutron star radius or the black hole's innermost stable circular orbit (ISCO), and  $R_0$  is the initial radius of the infalling material. Typically the initial radius is sufficiently high to make this right term negligible. For the neutron star, the energy released is roughly:

$$E_{\text{acc}} = 3.7 \times 10^{51} (m_{\text{acc}}/0.01M_{\odot}). \quad (5)$$

If the engine is 3% efficient at converting this energy into jet energy, accreting 1/10th of a solar mass would be sufficient to drive a  $10^{51}$  erg explosion. But to extract this energy and drive a jet, an accretion disk must form around the neutron star to wind up the magnetic fields. The BH accretion disk model releases more potential energy than the NS model, but extracting the energy might be more difficult. For these BHAD models, the disk is required to prevent the material from flowing directly into the black hole. Although accreting NSs need not form a disk to produce a jet, most engines require the formation of an accretion disk to produce the strong magnetic fields believed to produce relativistic jets.

For all three models, the formation of GRB jets is based on analogies with other astrophysical phenomena and not direct simulations. For example, although no simulations exist that produce highly-relativistic jets from magnetars (indeed, there is a known issue of baryon loading for magnetar jets in newly formed neutron stars Murguía-Berthier et al. [2014]), we know that normal pulsars produce energetic jets and it is plausible to assume that the higher-power jets in magnetars will have higher Lorentz factors. Similarly, current magnetohydrodynamic calculations have produced jets and we know that jets are produced in active galactic nuclei accretion disks. These calculations push the limit of current capabilities and it is not surprising that no calculation has captured this physics completely. However, it is plausible to assume that the more extreme accretion scenarios discussed for GRB progenitors will produce higher-Lorentz factor jets.

All three models successfully explain the energetics if the engine has sufficient angular momentum. Different progenitors produce different angular momentum profiles and we will discuss this in detail in Section 4. But to get a flavor of the issues tying energetics to our engines, let us review single star models and the kinds of angular momenta they produce. Figure 1 shows the angular momentum profile (specific angular momentum versus enclosed mass) for stellar-evolution models using 3 different prescriptions for the magnetic dynamo developed between burning layers in the star. On top of these profiles is plotted the angular momentum needed to form a disk at 1000 km. The angular momentum is lowest in the center of the star. The fact that the angular momentum increases with mass coordinate led scientists [Woosley, 1993,

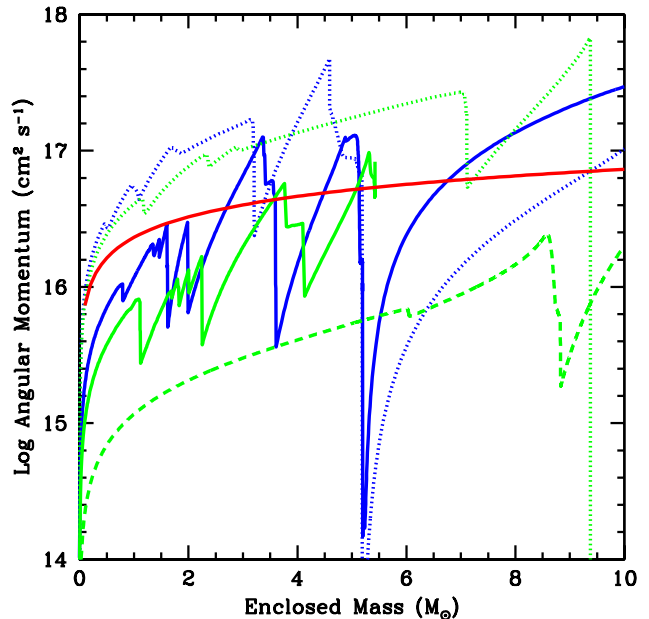


**Fig. 1.** Angular momentum profile (specific angular momentum versus of enclosed mass) for two different stellar models:  $15 M_{\odot}$  (blue),  $25 M_{\odot}$  (green). The dotted lines correspond to models using the GENEC code with no magnetic dynamo [Belczynski et al., 2017], the solid lines correspond to models using the Kepler code using a weak magnetic dynamo [Heger et al., 2005], and the dashed line corresponds to simulation using a stronger magnetic dynamo using the MESA code [Paxton et al., 2013]. The solid red line corresponds to the angular momentum needed to make a 1000 km disk around the compact remnant.

Fryer et al., 1999a] to argue for black hole accretion disk models over neutron star models. For the stellar models without any dynamo (dotted lines), the specific angular momentum is high, forming a disk whether the compact remnant formed is a neutron star or black hole. The neutron star spin would be less than a sub-millisecond and a potential magnetar model would be able to tap  $10^{52}$  erg of rotational energy. However, with even a weak dynamo (solid lines), a disk only forms once the compact remnant exceeds  $3 M_{\odot}$ . Such stars could not produce a NSAD engine. For the magnetar model, these stars would produce a millisecond neutron star, requiring efficiencies in excess of 25% to produce a  $10^{51}$  erg explosion for the magnetar model. For stronger magnetic dynamos, the angular momentum is too low to produce a disk around any compact remnant (NS or BH) and the neutron star is not spinning sufficiently rapidly to produce a GRB. Clearly, whether or not any engine works depends upon the angular momentum and it is not clear that stars can produce GRBs without some method to spin them up.

Angular momentum is a requirement for all the engines considered in this paper. As we shall see in our studies of disk models (Section 4), different progenitors produce different angular momenta and, hence, will have different observational properties (Sections 5,6).

## 4 Progenitors

Although the engines behind all of these models are different, the basic progenitors have similar features: a compact remnant with high angular momentum. In this section, we will review these progenitors, focusing on two broad progenitor classes: ones involving massive stars or ones involving the merger of two compact remnants.

### 4.1 Massive Star Progenitors

Massive star models made the first prediction confirmed by observations: the association of a supernova with long-duration gamma-ray bursts. For massive star models, the GRB jet is expected to drill through the star and, at the same time, eject the entire star, producing a supernova-like outburst [MacFadyen and Woosley, 1999]. No matter how a star is disrupted, whether it be a classic supernova explosion or a jet-driven outburst, an optical display will occur that peaks roughly 10-30 days after the explosion. This is simply a consequence of the evolution of the photosphere through the hot ejecta as it expands. Although additional power sources ( $^{56}\text{Ni}$  decay or magnetar) can augment this emission, the supernova-like light-curve will occur with or without this additional power source. With the observation of supernova 1998bw associated with GRB 980425 [Galama et al., 1999], massive stars became the likely candidate for some GRBs and theorists argued that many long GRBs should have these supernova-like outbursts.

Less than 0.1% of all stellar collapses produce gamma-ray bursts [Fryer et al., 2007, Sun et al., 2015, Levan et al., 2016]. One aspect of a progenitor model for GRBs is that the system must normally *not* produce a GRB, i.e. it is rare. Based on our current understanding of supernovae and the initial mass function, roughly 10% of all massive stars that undergo core-collapse form black holes [Fryer and Kalogera, 2001], so even this scenario must only work 1% of the time. The explanation for the rarity of these systems has been that it is difficult to achieve sufficient angular momentum to form a disk or rapidly-rotating magnetar. In the accretion disk models, if there is insufficient angular momentum, a disk isn't formed and the engine fails. The magnetar engine predicts a continuous range of drives with different spins. Superluminous supernovae may be examples of magnetars spinning too slowly to form a GRB [Kasen and Bildsten, 2010, Metzger et al., 2015]. Another clue to the progenitor may be that, thus far, all supernovae associated with GRBs appear to be type Ic supernovae<sup>1</sup>. Progenitor models, some favoring NS or BH formation, include:

- GRBs only form from the stars with the fastest birth spin rates. Fast rotation can cause strong mixing between layers, possibly causing the complete burning of the hydrogen and helium layers [Yoon and Langer, 2005]. This mixing, and hence homogenization, of the

star tends to only occur in rapidly rotating stars. It increases the core mass of massive stars, tending to produce black holes directly (producing the BHAD engine).

- Spin up by extremely close binaries. Stars in close binaries undergo mass transfer and, in many cases, an expanding star envelopes its companion, causing a common envelope phase. The common envelope phase tightens the orbit. Tidal interactions often spin down the stellar cores but, if the orbit is sufficiently tight, tidal locking can spin up the stars [van den Heuvel and Yoon, 2007]. With a weak or no dynamo slowing down the spin, all 3 (magnetar, NSAD, and BHAD) engines may be produced in this progenitor.
- In a subset of close binaries, the stars undergo a second common envelope phase prior to the collapse of the fastest-evolving star and, in a subset of these systems, this causes the two helium cores to merge, producing a rapidly rotating core [Fryer and Heger, 2005]. With a weak or no dynamo slowing down the spin, all engines may work.
- In a subset of systems where the fastest-evolving star collapses before its companion expands off the main sequence, the compact object can merge to the core of its companion, the perhaps poorly-named helium-merger scenario [Fryer and Woosley, 1998b, Zhang and Fryer, 2001]. High accretion rates in this scenario probably bury any magnetic field, so this model can only produce disk engines. The accretion rate will bury a magnetar magnetic field, but before the compact remnant collapses to form a BH, the NSAD may work. The BHAD disk will work for this system.

Achieving sufficient angular momentum is the driver behind all of these scenarios. For massive stars, the evolution of the magnetic field in the core depends both on the coupling of different stellar layers through, for example, a magnetic dynamo [Heger et al., 2005], or through mass loss from winds. Mass loss depends upon metallicity, and there is a tendency to argue that angular momentum loss from winds is higher at higher metallicities where mass loss from winds is highest, but anisotropies in this mass loss make it both difficult to determine the total angular momentum loss and the dependence of this angular momentum loss on winds [Georgy et al., 2013a, Gagnier et al., 2019]. For all but the last scenario, our current understanding of the magnetic dynamo makes it difficult to get high enough angular momentum profiles for the magnetar or neutron star accretion disk models to work. Indeed, it is difficult for these models to work even for the black hole accretion disk scenario. But it could be the progenitor is just that rare case where coupling does not occur. Ruling out a scenario is difficult when the event rate is as rare as the GRB event rate. The helium-merger model is the only current model that definitively produces sufficient angular momentum.

At this time, none of the models can easily explain the fact that all of the supernovae associated with GRBs are type Ic [Fryer et al., 2007]. Enhanced mixing models have argued that massive stars are more likely to homog-

<sup>1</sup> Type Ic are characterized by having no helium lines in their spectra - suggesting little or no helium in the ejecta

**Table 1.** Which Progenitors Work For Each Engine: “no dyn”  $\equiv$  the model works if there is no dynamo (or other viscous force) coupling the burning layers, “weak dyn”  $\equiv$  the model works even if there is some coupling between burning layers, “acc” refers to the accretion rate. Note that magnetar engines require that the magnetic field not be buried.

Progenitor	Magnetar	NSAD	BHAD
Rotating Star	no	no	weak dyn
Tidal Locking	no dyn	no dyn	weak dyn
He-He merger	no dyn	no dyn	weak dyn
He-merger	no	before BH	yes
WD/WD merger	yes	low acc	no
WD/NS merger	yes	low acc	BH?
WD/BH merger	no	no	low acc
NS/NS merger	yes	high acc	high acc
NS/BH merger	no	no	high acc

enize [Frey et al., 2013]. Black hole accretion disk models require more massive progenitors (otherwise the star forms a neutron star). These helium shells of these massive progenitors can undergo strong mixing and burn to carbon and oxygen. This is, perhaps, an explanation for the predominance of type Ic supernovae in GRBs. This explanation, however, only works for the BHAD engine.

Table 1 summarizes the possible massive-star progenitors and their potential engines. Whether or not the engines work depends upon the angular momentum in the massive star system. Magnetic fields are often invoked as the manner in which different burning layers are coupled, tying the angular momentum of the core to the outer layers of the star, slowing down the spin. In table 1, the strength of the magnetic dynamo determines this spin (the stronger the dynamo, the greater the coupling and the slower the spin).

## 4.2 Compact Mergers

Another class of models that produces the conditions for our GRB engines are the mergers of two compact remnants: BHs, NSs, or white dwarfs (WDs). For the magnetar model and NSAD engines, the merged remnant must be a NS (at least for some time after the merger) and for the BHAD, the remnant must ultimately become a BH. For the accretion disk models, a disk of material must remain behind to power the engine. These constraints rule out mergers of a BH/BH, but we discuss the other mergers here:

- WD/WD: Depending on the composition and merger process, the merger of two WDs may either ignite into a thermonuclear explosion (type Ia Supernova [Livio and Mazzali, 2018]) or collapse to form a neutron star (accretion induced collapse - AIC [Fryer et al., 1999b]). If it collapses, it can produce a dim, but fast supernova with an accretion disk around rapidly spinning neutron star [Fryer et al., 2009, Schwab, 2016]. This progenitor may work for either a NSAD or magnetar engine but

because it is very unlikely this merger will collapse to form a BH and it is not a viable BHAD progenitor.

- WD/(NS or BH): The merger of a white dwarf with either a neutron star or black hole will produce a large disk (roughly  $10^{10}$  cm in size) around a NS or BH remnant [Fryer et al., 1999c]. This merger could spin up a neutron star, producing a magnetar GRB (if the magnetic field is not buried or after the magnetic field resurfaces) [Metzger and Berger, 2012]. The accretion rate will be lower than other mergers for both NSAD and BHAD models.
- NS/NS: Neutron star mergers are one of the best-studied GRB models. The merger forms a rapidly spinning neutron star. The neutron star is extended ( $\sim 20$  km) after the merger but is spinning with  $\omega = 1500 - 2000 Hz$  [Ruffert and Janka, 1997, Rosswog and Ramirez-Ruiz, 2004, Rosswog, 2007, Fryer et al., 2015]. If the engine can tap 10-20% of the rotational energy, it could power a  $10^{51}$  erg burst. For accretion disk systems, disk properties dictate observable features. The disk is compact with a short lifetime (100 ms), but is expected to be high power (few times  $10^{51}$  erg) [Popham et al., 1999]. The high accretion rates and short duration are why theorists classified this as a short GRB progenitor [Fryer et al., 1999a, Popham et al., 1999].
- NS/BH: NS/BH mergers are similar to NS/NS mergers, but limited to the BHAD system. The power in NS/BH merger depends upon the mass and the black hole spin. The issue is that, especially for the more massive black holes, the tidal disruption of the neutron star occurs within the innermost stable circular orbit of the black hole [Janka et al., 1999, Ruffert et al., 2000, Shibata and Uryu, 2007]. Such systems will not form a GRB. Population synthesis calculations suggest that 1% of NS/BH mergers with low-spin black holes ( $a < 0.6$ ) form disks and 40% of high-spin black holes are able to form disks [Belczynski et al., 2008]. But these systems can form massive accretion disks, producing the most energetic short-duration GRBs.

Table 1 summarizes the possible merger progenitors and their potential engines. Obviously, which engine works depends upon the fate of the merged compact remnant: BH versus NS. For the magnetar engine, the merger must not lead to rapid accretion that buries the magnetic field preventing any outburst until the magnetic field resurfaces.

## 5 GRB Durations

The durations of our engines can be estimated analytically, providing constraints on which progenitors (with which engines) can explain the observed durations. In this section, we review these estimates.

For magnetar GRBs, the duration can be estimated using pulsar spin-down models that, in turn are approximate and depend upon assumptions of the particle acceleration in a pulsar. Models of increasing sophistication

exist [Contopoulos and Spitkovsky, 2006]:

$$L_{\text{pulsar}} = \frac{B^2 r_{\text{NS}}^6 \omega_{\text{NS}}^4}{4c^3} (\alpha_{\text{psr}} \sin^2 \theta + [1 - \omega_{\text{death}}/\omega_{\text{NS}}] \cos^2 \theta) \quad (6)$$

where  $B$  is the dipole magnetic field,  $r_{\text{NS}}$  is the neutron star radius,  $\omega_{\text{NS}}$  is the neutron star spin,  $\alpha_{\text{psr}}$  is the dipole spin-down efficiency,  $\omega_{\text{death}}$  is a function of the magnetic potential gap and the dipole magnetic field flux, and  $\theta$  is the alignment of the spin and dipole magnetic field axes. For rough estimates, many just take the leading terms, assuming  $\alpha_{\text{psr}} = 1$  and  $\theta = 90^\circ$ :

$$L_{\text{pulsar}} = \frac{B^2 r_{\text{NS}}^6 \omega_{\text{NS}}^4}{4c^3} \approx 10^{49} (B/10^{15} \text{G})^2 \text{erg s}^{-1} \quad (7)$$

for a 10 km, millisecond pulsar. The duration of such an engine is approximated by taking the ratio of the rotational energy to the pulsar power ( $T_{\text{magnetar}} = E_{\text{rot}}/L_{\text{pulsar}}$ ):

$$T_{\text{magnetar}} = 100 (r_{\text{NS}}/10 \text{ km})^{-4} (\omega_{\text{NS}})^{-2} B^{-2} \text{ s}. \quad (8)$$

The qualitative properties of magnetar-driven GRBs follows trends in the data: i.e., higher spin magnetars will produce shorter, but more powerful, GRBs, matching the long-soft, short-hard subclasses of bursts. But this engine struggles to match more detailed data. For example, it appears that the long bursts typically have more, not less, total energy, arguing that they are produced from faster, not slower, spinning magnetars (contrary to the prediction from our simple duration fit). To make the magnetar model fit all GRB populations, we will have to invoke more parameters and features. Astrophysicists also do not understand magnetic field generation enough to make strong predictions on which progenitors make long versus short bursts or even why there is a bimodal distribution of durations. Simply put, the magnetar model struggles to explain current data on GRB durations and, although the uncertainties allow it to fit the current data, the parameters are so poorly known that it can not make firm predictions about different properties of short and long bursts.

The disk models are better understood, making firmer predictions. The duration of the disk models is set by the lifetime of the disk. If the disk is not continuously fed, the duration is the lifetime of the disk. If we assume an  $\alpha$  disk, the lifetime of the disk ( $T_{\text{disk}}$ ) can be estimated by the orbital period of the maximum extent of the disk divided by  $\alpha$ :

$$T_{\text{disk}} = (2\pi r_{\text{disk}}^{3/2}) / (G^{1/2} M_{\text{rem}}^{1/2} \alpha) \quad (9)$$

where  $r_{\text{disk}}$  is the radius of the disk,  $G$  is the gravitational constant, and  $M_{\text{rem}}$  is the remnant mass. For a disk formed from material with specific angular momentum  $j$ , the timescale for the disk accretion is:

$$\begin{aligned} T_{\text{disk}} &= (2\pi j^3) / (G^2 M_{\text{rem}}^2 \alpha) \\ &= 4(j/10^{17} \text{cm}^2 \text{s}^{-1})^3 (3M_{\odot}/M_{\text{rem}})^2 (0.01/\alpha) \text{ s}. \end{aligned} \quad (10)$$

For a typical neutron star merger, the disk lifetime is roughly 100ms, fitting the average timescale of short-duration

bursts. For helium-merger models, the specific angular momentum can be  $10^{18} \text{cm}^2 \text{s}^{-1}$ , producing very long (more than 1000 s) GRBs. With the discovery of weak, ultra-long bursts, interest in the He-merger progenitor has increased.

This disk accretion timescale is appropriate for compact mergers where there is no way to feed the disk. But for massive stars, the disk is replenished by further accretion onto the disk from the star which continues either until the star is disrupted or it completely accretes onto the compact remnant. The free-fall time ( $T_{\text{free-fall}}$ ) of the star onto the compact remnant places an upper limit on the duration of the engine:

$$\begin{aligned} T_{\text{free-fall}} &= \pi r_{\text{star}}^{3/2} / (8GM_{\text{star}})^{1/2} \\ &\approx 35 \text{ s} (r_{\text{star}}/10^{10} \text{ cm})^{3/2} (8M_{\odot}/M_{\text{star}})^{1/2} \end{aligned} \quad (11)$$

where  $r_{\text{star}}$  is the radius of the stellar He or CO core and  $M_{\text{star}}$  is the mass of this core. Depending upon the compactness of the core, the timescale for CO core collapse can be as high as a few hundred seconds. For longer-lived GRBs, the star must include part of the helium layer, a problem if these ultra-long bursts also only have associated type Ic, instead of Ib, supernovae.

Popham et al. [1999] reviewed different progenitors, their durations and their power (energy deposited per unit time -  $\text{erg s}^{-1}$ ). Since this time, better models for the disks have been produced and we can use these models and the Popham et al. [1999] analysis to estimate powers and durations of the different progenitors. Table 2 shows the power and durations for the progenitors in this study combining analytic prescriptions, disk models and our current understanding of the progenitor evolution. The prediction is the same for the massive star models at this time, because the models are not yet sufficiently detailed to differentiate the progenitors. For massive stars, the lower time limit is set by the time the jet requires to punch through the star ( $\approx R_{\text{star}}/c \sim 1 \text{ s}$  for C/O cores). The upper limit is set by the infall time of a C/O core or, in the case of NSAD models, the collapse time of the neutron star.

## 6 Progenitor/Engine Predictions

Aside from the association between long duration GRBs and supernovae, most of the constraints we have discussed thus far are “post-dictions”; that is, theorists ensuring that their models fit existing data. The different progenitor and engine models have made a series of predictions. For some engines, the subsequent observations begin to rule out some engines. For others, the observations have been confirmed, strengthening the case for these models/engines.

### 6.1 Magnetar Engines and Late-Time Emission

Because we know very little about the neutron star spin and magnetic fields, it is difficult to tie progenitors to predictions about the magnetar engine. As we mentioned in the discussion on durations, we do not understand the

**Table 2.** Durations and Power for Accretion Disk Models

Progenitor	Power	Duration
<b>BHAD Models</b>		
Rotating Star	$\sim 10^{50} \text{ erg s}^{-1}$	1 – 300 s
Tidal Locking	$\sim 10^{50} \text{ erg s}^{-1}$	1 – 300 s
He-He merger	$\sim 10^{50} \text{ erg s}^{-1}$	1 – 300 s
He-merger	$\sim 10^{50} \text{ erg s}^{-1}$	300 – $10^4$ s
WD/BH merger	$\sim 10^{49} \text{ erg s}^{-1}$	300 – $10^4$ s
NS/NS merger	$\sim 10^{51} \text{ erg s}^{-1}$	< 1 s
NS/BH merger	$\sim 10^{51} \text{ erg s}^{-1}$	< 1 s
<b>NSAD Models</b>		
Rotating Star	$\sim 10^{50} \text{ erg s}^{-1}$	1 – 10 s
Tidal Locking	$\sim 10^{50} \text{ erg s}^{-1}$	1 – 10 s
He-He merger	$\sim 10^{50} \text{ erg s}^{-1}$	1 – 10 s
He-merger	$\sim 10^{50} \text{ erg s}^{-1}$	300 – $10^4$ s
WD/WD merger	$\sim 10^{49} \text{ erg s}^{-1}$	300 – $10^4$ s
WD/NS merger	$\sim 10^{49} \text{ erg s}^{-1}$	300 – $10^4$ s
NS/NS merger	$\sim 10^{51} \text{ erg s}^{-1}$	< 1 s

generation of magnetic fields well enough to tie strong magnetic fields to particular progenitors. But the magnetar model does make predictions based on the engine alone. If a magnetar is driving the GRB, there should be late-time emission in the afterglow (e.g. radio) (unless the star collapses to a black hole). This emission is not seen in short bursts [Fong et al., 2016], arguing against the magnetar engine for these bursts. In addition, observations from GW170817 also have shown that no magnetar existed at late times although it is possible the magnetar collapsed to a black hole after driving a jet or that a normal field ( $10^{12}$  Gauss) neutron star exists in this merger [Piro et al., 2019]. It is clear that the magnetar engine must overcome some challenges to explain the current set of short-duration GRB observations.

## 6.2 Distributions of Disk Engines

Because we can tie properties of the accretion disk models to specific progenitors, we can use our understanding of these progenitors to make predictions on further properties of these models. As we discussed in section 5, short-duration GRBs are expected to arise from NS/NS and NS/BH mergers. Long bursts are expected to arise from massive star models, He-mergers or WD/(BH or NS) mergers. But the bulk of long bursts are expected to arise from massive stars. Within this framework, scientists began to make predictions for different bursts: long bursts should form in star-forming galaxies whereas short bursts should occur in all galaxy types.

Theory made further predictions based on the accretion disk paradigm. If short bursts are only produced by NS/NS and NS/BH mergers, the kicks imparted onto NSs at formation cause these binaries to be ejected from their star forming regions (and, in some cases, even their host galaxies). Theorists made predictions for the distribution of offsets of these mergers [Fryer et al., 1999a, Bloom et al., 1999], arguing that short duration GRBs should be much

more spatially extended than supernovae. If the BHAD engine is correct, long-duration bursts should form from the most massive stars, located close to young star forming regions.

A growing set of observations seem to support this paradigm: long bursts appear to be concentrated near the peak emission in star-forming galaxies, are even more centrally located than supernovae [Vreeswijk et al., 2001, Bloom, 2003, Fruchter et al., 2006]. Full confirmation of the accretion disk paradigm required observations demonstrating short GRBs arise from mergers, e.g. a large offset distribution. The Swift satellite pinpointed the position of short GRBs sufficiently to allow good follow-up observations of these bursts, proving that short-duration bursts were not only more distributed than their counterparts, but some were found that are outside their host galaxy [Fong et al., 2013, Fong and Berger, 2013].

GW170817 cemented the neutron star merger scenario for short bursts, but the observations were more detailed than is often realized. The gravitational wave detection [Abbott et al., 2017] proved that a compact merger (from the inferred masses, a NS/NS merger) event occurred. The corresponding gamma-ray observations [Savchenko et al., 2017] showed that gamma-rays did arise from this merger. X-ray afterglow observations, e.g. [Troja et al., 2017], suggested an off-axis GRB and the radio argued strongly for the presence of a relativistic jet [Mooley et al., 2018]. All the evidence together argues strongly that GW170817 was a true short GRB from a neutron star merger.

By assuming the accretion disk paradigm is behind GRBs, astrophysicists can predict which progenitors are behind different types of bursts: massive stars dominated the progenitors of long bursts and NS/NS and NS/BH mergers produce short bursts. The prediction of this paradigm allowed astronomers to use population characteristics of the different burst types to either confirm or rule out this engine. The subsequent 20 years of observations, including the recent GW170817 observations, have supported the predictions of this engine. With such a strong confirmation, the accretion disk paradigm remains the leading GRB class of engines.

## 6.3 Mergers and the r-Process

During the merger, matter is ejected both during the tidal disruption of the neutron star(s) and through winds during the subsequent disk accretion onto the core [Metzger and Berger, 2012]. The neutron-rich dynamical ejecta from BH/NS and NS/NS mergers were suggested as possible r-process sites [Lattimer and Schramm, 1974]. In addition to playing an important role in the synthesis of heavy elements in the universe, this ejecta produces a fast transient. Like a thermonuclear supernova, the decay of the neutron-rich, radioactive isotopes produced in these mergers can power a transient from which we can probe the ejecta properties. Several potential infra-red detections were made prior to GW170817 [Berger et al., 2013, Tanvir et al., 2013], but many of these detections had corresponding X-ray flares, suggesting a shock interaction instead of



a true kilonova observation [Kasliwal et al., 2017]. The optical and infra-red observations of GW170817 provided the first definitive observation of the ejecta from neutron star mergers.

Before we discuss the results of the observations, let us review what was known from theory. Simulations demonstrated that the tidal ejecta were sufficiently neutron rich to produce heavy r-process [Freiburghaus et al., 1999, Goriely et al., 2011, Roberts et al., 2011, Korobkin et al., 2012, Richers et al., 2015, Montes et al., 2016, Sekiguchi et al., 2016, Radice et al., 2016, Shibata et al., 2017, Bovard et al., 2017, Foucart, 2018]. Scientists found that the total amount of neutron-rich ejecta depends upon the relative neutron star masses of the two compact remnants [Korobkin et al., 2012]. However, uncertainties in the simulations (e.g. implementation of the physics and numerical artifacts) are fairly large and the results from current calculations range from  $0.001 - 0.05 M_{\odot}$ . NS/BH mergers have a much wider range of dynamical ejecta masses ranging from no ejecta whatsoever when the the black hole is large and the neutron star is tidally disrupted within the innermost stable circular orbit up to  $\sim 0.1 M_{\odot}$  for smaller-mass black holes.

Some basic trends exist with the disk ejection. If the remnant remains a neutron star, “wind” ejecta includes both disk winds and accretion outflows (on par with the re-ejection of mass in supernova fallback [Fryer, 2009]) [Metzger and Berger, 2012]. If the remnant is a BH, this latter outflow does not occur and we expect more ejecta from systems with NS cores than those with BH cores. Neutrinos can reset the neutron fraction in the ejecta to equal numbers of neutrons and protons and it is believed that systems with NS cores (and their resultant neutrino flux) will be reset further than those with BH cores. But just as with the dynamical ejecta, physic implementation and numerical artifacts dominate the solutions, and the wind ejecta masses range from  $0.001 - 0.05 M_{\odot}$  with electron fractions  $[Y_e = n_e/(n_e + n_n)]$  where  $n_e, n_n$  are the numbers of electrons and neutrons respectively] ranging from slightly above dynamical ejecta (0.1-0.25 to 0.35-0.4). The electron fraction plays a major role in dictating the yields<sup>2</sup>. For high electron fractions, the ejecta does not produce heavy r-process elements, and the ejecta can be dominated by iron peak elements. At this time, simulation differences are larger than the trends.

Calculating the electron fraction, and hence final yields, from the late-time wind ejecta depends upon many modeling and physics uncertainties including neutrino transport and its coupling to the hydrodynamics, magnetic fields, dense nuclear equations of state and neutrino physics. Al-

<sup>2</sup> The yields of any explosive event depend upon the electron fraction, the entropy and the density/temperature evolution [see, for example Lippuner and Roberts, 2015, Magkotsios et al., 2010]. The density/temperature profiles are generally well fit by analytic profiles. For the variations of these parameters in neutron star mergers, these latter two parameters do not have as strong an effect as the electron/neutron fraction on the broad r-process yields. However, all three must be understood to produce exact yields.

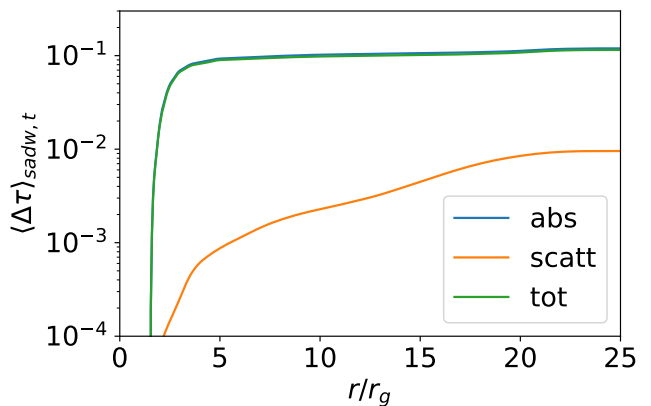


**Fig. 2.** Average absorption, scattering, and total optical depth that a neutrino emitted in the inner region of a post-neutron-star-merger disk passes through as a function of distance from the black hole in gravitational radii. The optical depth is averaged both over spherical shells at each radius and over time, from 20ms to 27ms in a two-dimensional simulation.

though the number of models of this wind ejecta continues to increase [Foucart et al., 2015, Hossein Nouri et al., 2018, Siegel and Metzger, 2018, Fernández et al., 2018, Miller et al., 2019], these uncertainties still produce ejecta with a wide range of electron fraction. To understand the extent of these uncertainties, we study just one aspect, the neutrino transport. Figure 2 shows the average absorption, scattering, and total optical depths that a neutrino emitted in the inner region of a post-neutron-star-merger disk passes through as a function of distance from the central black hole from a disk model using the  `$\nu$ bhlight` code [Miller et al., 2019]. A vanishing optical depth would imply that optically thin cooling is appropriate, whereas an infinite optical depth would imply neutrinos never escape. Although the disk is optically thin, the optical depth is not negligible. Free-streaming will not capture all of the physics.

Figure 3 shows the electron fraction of the ejecta from a black hole accretion disk using the  `$\nu$ bhlight` code, both with neutrino transport (using Monte Carlo methods) and a free streaming prescription. The left panel shows the electron fraction using full transport, accounting for absorption, emission, and scattering. With full transport, the electron fraction varies dramatically in space, reaching relatively large values. The right panel shows the electron fraction if one instead assumes optically thin cooling, with no absorption or scattering. With only cooling, the electron fraction is universally low and the outflow is extremely neutron rich. These two outflows may produce dramatically different nucleosynthetic yields. These will produce different light-curves and contribute differently to the r-process.

The combination of both neutron rich dynamical ejecta (producing the r-process) and neutron poor wind ejecta led theorists to predict two components in the light curve [Metzger and Fernández, 2014]. Ultraviolet, optical and infra-red observations of this ejecta can be used to deter-



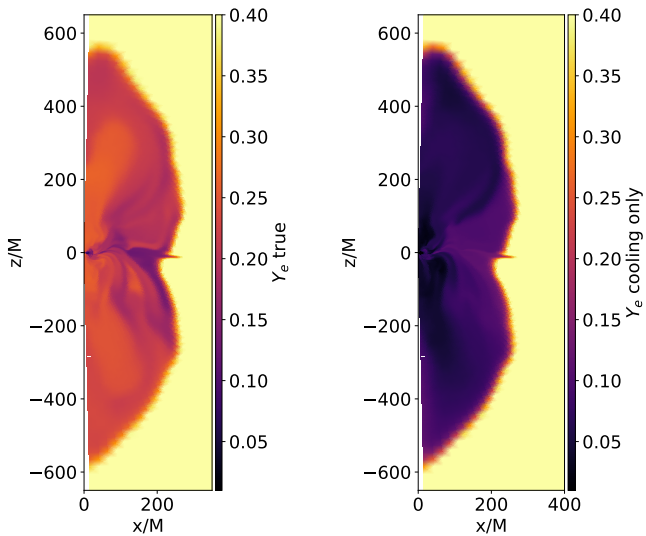


**Fig. 3.** Electron fraction in the outflow after 27ms from a two-dimensional simulation of a post-neutron-star-merger disk. Left: electron fraction if one solves the Boltzmann equation for the neutrinos. Right: electron fraction if one assumes optically thin cooling and no absorption.

mine the relative fractions neutron-rich material. Unfortunately, GW170817 has demonstrated just how difficult it is to produce firm ejecta masses from the light-curves and the range of ejecta masses fit to the observations are nearly as large as the uncertainties in the models [Côté et al., 2018a]<sup>3</sup>. In addition to the ejecta mass, the light-curve depends upon the opacities and their coupling to transport, understanding of aspects of the ejecta (morphology, velocity and density distributions, exact composition, ...), and other energy sources. For example, although, as mentioned above, we can show that GW170817 does not have a long-lived magnetar, observations do not rule out a long-lived pulsar [Piro et al., 2019]. Such a pulsar will affect the early time emission. Figure 4 shows the bolometric light curve of GW170817 matched by two different models: a massive wind (high electron fraction) ejecta ( $0.03 M_{\odot}$ ) simulation and a low-mass wind ejecta ( $0.001 M_{\odot}$ ) with a  $10^{12}$  G pulsar simulation. Both fit the observations, but the difference in ejecta mass is a factor of 30. Without detailed modeling (hopefully identifying discriminating observables), what we can learn from even multi-diagnostic signals is limited. But some general trends exist: if the remnant remains a neutron star, the neutrinos from this neutrino star will raise the electron fraction of the ejecta, tending to produce more iron peak and 1st r-process elements. This produces a stronger optical/UV signal, especially in the first day or two after the merger. If the core collapses to a black hole, the electron fraction is lower producing heavier r-process elements whose opacities make a redder transient.

Whether or not mergers can be the dominant source of the r-process depends both on the rate of these mergers

<sup>3</sup> Perhaps not surprising given the difficulty in estimating supernova ejecta masses from light-curves and spectra.

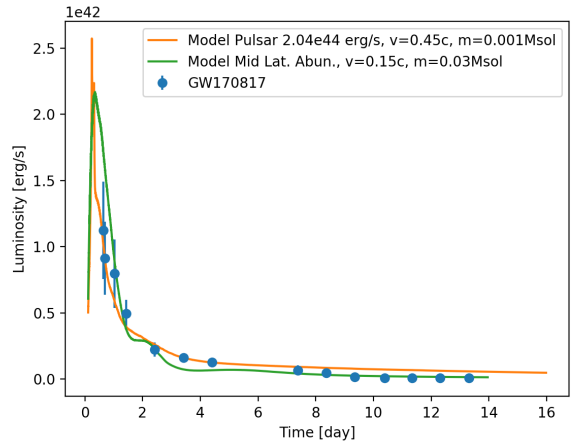


**Fig. 4.** Bolometric luminosity versus for two different kilonova models: the W2 wind model [Wollaeger et al., 2018] with  $0.03 M_{\odot}$  of wind ejecta (high electron fraction) moving at 0.15 the speed of light, and a wind model with  $0.001 M_{\odot}$

and the amount of neutron-rich ejecta [Côté et al., 2017]. Prior to GW170817, the strongest constraints on the rate of compact mergers came from observations of close binary pulsar systems. Pulsar binaries like the Hulse-Taylor pulsar could be used to estimate the rate of mergers [Kalogera et al., 2004]. But selection effects (beaming, recycling efficiencies, kicks) made it difficult to place strong constraints on the rate. Assuming mergers produce short GRBs, astrophysicists could also predict a merger rate but, again, biases (uncertain beaming) made it extremely difficult to determine an accurate rate [Chen and Holz, 2013]. Theory is equally uncertain. Errors in the rate that span many orders of magnitude, allowing the potential for mergers to either dominate the r-process production in the universe to scenarios where mergers make up only a few percent of the r-process in the universe [Fryer et al., 1999a, Dominik et al., 2012]. The observational uncertainties from gravitational wave detections are much smaller and, even though GW170817 is only one event, it is already placing among the most stringent constraints on neutron star merger rates and the role of mergers in producing the heavy elements in the universe [Côté et al., 2018b].

## 7 For the Future

There is no doubt that GW170817 dramatically improved our understanding of short-duration GRBs. Neutron star merger rate estimates based on GW170817 are the most stringent to date. Coupled with optical and infra-red observations, GW170817 provided the first definitive evidence of ejecta from the merger. Coupled with gamma-ray, X-ray and radio observations, GW170817 places some of the strongest evidence that mergers produce GRBs. In all cases, GW170817 is adding to the 50-year set of data that has led scientists to the current standard models behind GRBs. We conclude with a description of what the future holds for GRB observations.

## 7.1 Understanding GRB Properties

Gravitational waves have already made a major contribution to our understanding of short duration gamma-ray bursts. Gravitational wave detections alone will be able to pinpoint the NS merger rate over the next few years. The biggest uncertainty in the rate estimate from GW170817 is the fact that, at this time, we have only one event. However, as aLIGO becomes increasingly sensitive, the rate of merger detections will increase (although it may get more difficult to obtain data across the electromagnetic spectrum) and the sample of NS/NS and even NS/BH should grow dramatically with time. aLIGO alone will tightly constrain the rate of mergers.

Multi-messenger astronomy enhances the science we can learn. As we build up our observational database of merger detections with concurrent gamma-ray measurements, we will improve our understanding of gamma-ray bursts. For example, if we can pin down mergers as the primary source of short-duration GRBs, we can use the rate of mergers to constrain the beaming of these outbursts. A broader set of diagnostics will help us study the jet in more detail, i.e. the gravitational wave signal and the kilonova signal place limits on the viewing angle (the angle between the orbital angular momentum axis and our line of sight) of the burst. GW170817 provided a first probe of the off-axis structure of the jet producing the gamma-ray burst. As we build up our sample of well-studied mergers with a range of viewing angles, we can probe in detail the GRB jet structure.

Coupled with UVOIR measurements, LIGO detections will also grow the sample of ejecta detections. As we discussed in section 6.3, the UV, optical and infra-red measurements are produced by the ejecta in neutron star mergers and observations of this kilonova have been used to determine the characteristics of this ejecta. Unfortunately, uncertainties in this modeling make it difficult, with one event, to pinpoint the exact yields and, currently, a range of results exist for the broad set of analyses [Côté et al., 2018a]. However, as the number of events increase and the models improve, scientists will be able to break the current degeneracies, obtaining more exact yields. This information can be applied to events beyond the LIGO detection threshold. For example, scientists have taken the properties optical and infra-red emission (arising from decay energy in the ejecta) to see if any other GRBs have similar properties [Rossi et al., 2019]. As we detect more nearby events (with joint gravitational wave and electromagnetic wave signals), we can determine the range of emission arising from these mergers. Coupled with detailed models, these observations can probe the characteristics (velocities, density distribution, and composition) of the ejecta. These studies will determine the role mergers play in producing r-process elements in the universe and provide a much more detailed picture of r-process production. With detailed ejecta and light-curve models, astrophysicists will be able to differentiate NSAD and BHAD engines. And, as we shall discuss below, by determining the fate of the core, we probe the behavior of matter at nuclear densities.

Bear in mind these studies rely on a basic understanding of the physics behind these outbursts and modelers must deal with both physics and numerical uncertainties. For example, the exact nature of the nuclear physics can alter the yield, changing the energy deposition and the light-curve (for the same ejecta mass) [Zhu et al., 2018]. Understanding and minimizing the nuclear physics uncertainties that affect the optical and infra-red light-curves are essential to using observations to constrain ejecta properties. Other physics effects are also important. In section 6, we already reviewed many of the uncertainties: additional energy sources, opacities and opacity implementations into transport, ejecta properties, neutrino and nuclear physics. Considerable multi-physics work is necessary to fully take advantage of the upcoming data.

Gravitational waves, by themselves, can be used to probe the neutron star equation of state. But as the number of well-studied (with gravitational wave and broad electromagnetic coverage) events increase, we can further probe the properties of this equation of state [Fryer et al., 2015]. These probes rely upon detailed models studying the regularization of the angular momentum (it is believed that the gradients in spin will disappear in the core) and the neutrino cooling will quickly reduce the thermal pressure. Comparing different electromagnetic signals from these mergers, coupled with gravitational wave constraints on the NS component masses, can probe the maximum neutron star or black hole mass.

Gravitational waves have the potential to place strong constraints on the engines and physics behind long-duration gamma-ray bursts. But, for most of the long-duration GRB progenitors, the gravitational wave signal is likely to be much weaker than neutron star merger progenitors. For massive star progenitors, signal is likely to be similar to those of supernovae which, for the most part, produce signals that are only detectable for events occurring in the Milky Way [Fryer and New, 2011]. For the engine to work, the rotation of these systems must be high and this can lead to higher gravitational wave signals that may, with next generation detections, be detectable out to the Virgo cluster [Fryer et al., 2002, Fryer and New, 2011]. For progenitors invoking mergers with helium stars or white dwarfs produce low-frequency signals in the LISA band, but will also only be detectable in the Milky Way. Given the rarity of these events, it is unlikely that gravitational-wave detectors will detect a long-duration burst in the near future. However, if such a detection would occur, gravitational waves would be an ideal probe of the details of the progenitor: progenitor scenario and its characteristics.

## 7.2 Predictions with Redshift

By increasing our understanding of the properties of GRBs, we can begin to use these powerful explosions to probe the early universe. But first, we must understand the evolution of these bursts with redshift. One of the primary differences in the evolution of progenitors with redshift is the difference in the amount of metals. One of the exciting

prospects of well-studied events in the nearby universe is to use them to study metallicity effects so that we may make predictions for these high redshift bursts.

Metals are important for cooling gas in star formation. Some cosmological models argued that stars without this cooling would not form binaries, arguing population III stars could not form the binary progenitors needed to produce GRBs, decreasing the fraction GRBs at high redshift [Belczynski et al., 2010]. However, once numerical issues with the ENZO code were fixed [Passy et al., 2012], their population III stars began forming binaries. Even so, it is still believed that lower cooling will lead to more massive stars, on average, possibly flattening the initial mass function which would increase the fraction of GRBs at high redshift [Lloyd-Ronning et al., 2002, Pescalli et al., 2016]. Absorption from metals can also lead to larger giant envelopes and increased mass loss, especially for stars with hydrogen envelopes. For long bursts, Young and Fryer [2007] used these differences to predict the distribution of GRBs as a function of redshift for different progenitors. A similar study for short bursts was done by Dominik et al. [2013].

The past studies folded prescriptions for metallicity evolution as well as prescriptions for stars and star formation, typically focusing on rates. Well-studied nearby systems (that include both gravitational wave and broad spectral data) can be used to probe the variation in GRB properties as a function of metallicity. In this section, we will discuss the current predictions for this evolution. For each progenitor, Fryer et al. [1999a] studied the rate dependence on the initial mass function, the stellar radius, and mass loss. From this study, we can calculate a broad set of GRB properties as a function of redshift: duration, power, circumstellar properties and the rate. Especially for merger events, timing (tighter mergers merge more quickly) can also alter the results and we will include these differences as well.

Before we review individual progenitors and their properties, let us review how the mass function, mass loss, and stellar radii effect stellar and binary evolution:

- **Initial Mass Function:** Cooling from metals allows smaller proto-stellar cores to collapse to form stars and the tendency is for these cores to produce lower-mass stars. Especially for Pop III stars, where this cooling is absent, we expect an initial mass function that is highly skewed toward massive stars. By itself, this suggests that a much larger fraction of stars will form GRBs at high redshift [Lloyd-Ronning et al., 2002]. Across all progenitor models (except for WD/WD mergers), the rate increases with a flattening of the IMF, but the rates of BH systems (black hole collapsars, BH/(NS,WD) mergers) increase more rapidly than NS systems [Fryer et al., 1999a].
- **Stellar Radius:** The amount of expansion in the giant phase of a massive star depends upon the opacity. Since metals dominate this opacity, higher metallicity stars will have larger radii. Figure 5 shows the radii (at collapse - this is not necessarily the maximum radius, but it is generally close to it) for 20 and 25  $M_{\odot}$  stars using

the GENEK [Ekström et al., 2012, Georgy et al., 2012, 2013b] and KEPLER [Woosley et al., 2002] as a function of metallicity. For the solar metallicity GENEK models, the radius is small because winds eject all of the hydrogen envelope. For models that retain their hydrogen envelope (all KEPLER models, models below solar metallicity with the GENEK code), the radius decreases with metallicity. This effect is most dramatic below roughly 1/100th solar metallicity. Many of the binary progenitors for GRBs require common envelope interactions to tighten the orbit. If the initial orbital separation is the same, decreasing the radius of the giant star will decrease the number of systems that undergo common envelope evolution, lowering the fraction of progenitors. However, this effect is muted by the fact that the widest separation systems undergoing common envelope evolution tend not to form GRB progenitors: e.g. for compact object progenitors, these wider binaries tend to get disrupted during compact object formation and/or remain wide and do not merge within a Hubble time.

- **Mass Loss:** Stellar winds are typically believed to be driven by atomic lines and higher metallicity stars have stronger winds. If the mass loss is sufficiently extensive to alter the mass of the stellar core at collapse, it can change its fate: e.g. the collapse can form a NS instead of a black hole. This is important for metallicities above 1/10th solar, but, below this metallicity, the mass loss from winds is minimal and does not play a major role in altering the fate of the massive star. But as the metallicity increases from 1/100th solar up to solar, the relative fraction of BH systems decreases and the fraction of NS systems increases.

We can now apply the trends with metallicity in the initial mass function, stellar radii, and mass loss to the specific progenitors in this paper:

- **Massive Rotating Star:** The rate of this progenitor as a function of the star formation rate, especially those forming BHAD engines, will increase with redshift because the initial mass function produces more massive stars and mass loss is limited. The cores of these stars might be slightly more compact, producing more powerful bursts, but this trend is not robust. Similarly, there is no obvious trend in the duration. The circumstellar medium (CSM) at high redshift will have wind profiles with lower mass loss rates surrounded by higher ambient densities (making smaller wind profile  $r^{-2}$  regions), but if common envelope evolution drives the mass loss of the hydrogen envelope and helium winds are less sensitive to metals, the CSM properties could be similar and not vary dramatically.
- **Tidal Locking:** The flattening of the IMF and lower winds will increase the rate of this progenitor. Although smaller radii might lower the rate, this scenario needs very close progenitors and is probably not strongly affected by the radius variations. More fast-spinning cores are likely to be produced with the more compact stars, possibly making stronger/longer bursts. Like all massive stars, the winds are weaker, but the

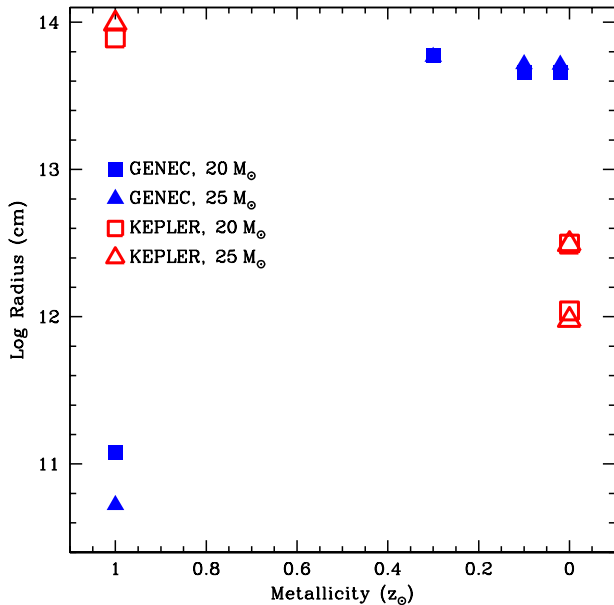


**Fig. 5.** Stellar radius at collapse for 20 and 25  $M_{\odot}$  zero-age main sequence stars as a function of metallicity for both GENE [Belczynski et al., 2017] and KEPLER [Woosley et al., 2002] codes. The GENE stars lose their entire hydrogen envelopes at solar metallicity, making compact helium stars. For all other models, the radii decrease with metallicity. The most dramatic effect occurs below roughly 1/100th solar metallicity. Population III stars will have radii that are more than an order of magnitude lower than stars at 1/10th solar metallicity.

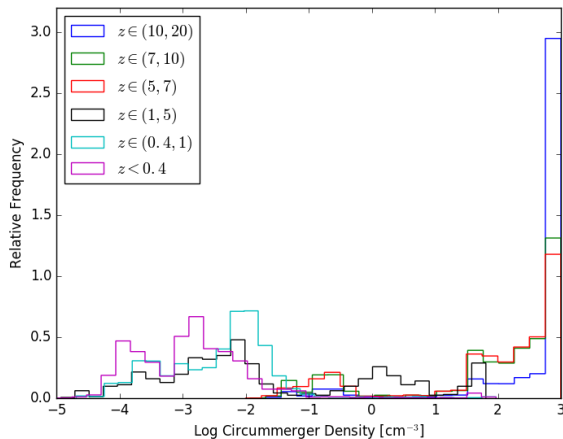


**Fig. 6.** Distribution of CSM densities as a function of redshift band for double neutron star mergers. Below a redshift of 1, there is a bimodal peak of the CSM density for these mergers. The low densities occur for binaries with long merger times where the systematic velocity can carry the binary well away from its formation site (and even beyond its host galaxy). The high densities occur for binaries with short merger times. The densities become increasingly higher at high redshift because the only systems that have merged at this time have short merger times and hence the systems are found preferentially in their high-density star forming regions.

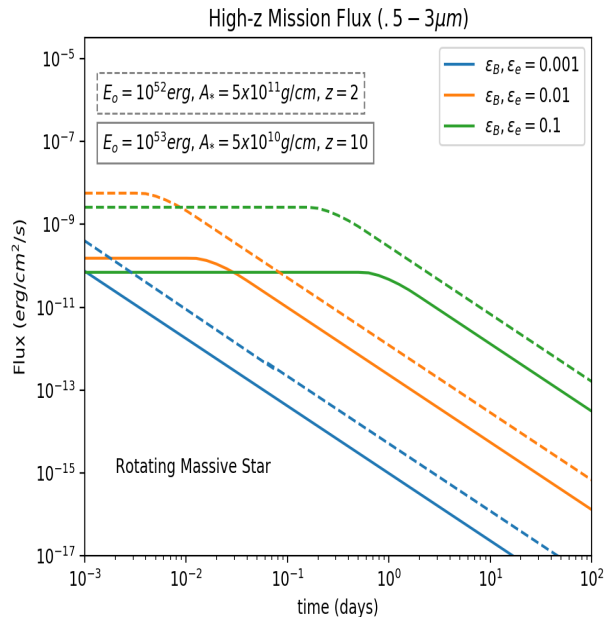


**Fig. 7.** Two fiducial lightcurves in the High-z bandpass for a rotating massive star models at a redshift of 10 (solid lines) and 2 (dashed lines) for different values of the fractions of energy in the electrons and magnetic field. The high redshift progenitor has less wind, but a higher isotropic emitted energy, while the lower redshift progenitor presumably has a stronger wind (due to higher metallicity) and a lower isotropic emitted energy.

ISM likely has higher densities (producing more compact wind bubbles).

- **He-He merger:** Typically larger helium cores in this progenitor could produce more powerful and longer bursts. These more massive helium cores will drive stronger winds within the possibly higher interstellar medium.
- **He-merger:** The merger rate of a helium star with a NS or BH companion will increase for the same reasons as the rest of our massive star models. Because the helium cores in these mergers will tend to be more massive, we expect these GRBs to be more powerful. The specific angular momentum of these mergers will probably balance out and not make significantly longer bursts, but recall that this progenitor has been invoked already to make ultra-long bursts. The CSM properties should mirror the rotating massive star models
- **NS/NS Mergers:** The rate of NS mergers stays roughly constant, but with slightly higher NS masses, the disk masses are likely to be higher, producing stronger bursts. More massive NSs are more compact, so the duration may be shorter. Wiggins et al. [2018] found that higher redshift mergers occurred in higher densities (both because shorter period binaries play a bigger role at higher redshift and because star-forming regions are denser. Figure 6 shows the predicted densities for mergers as a function of redshift band. This effect will be true for all of the compact merger events.

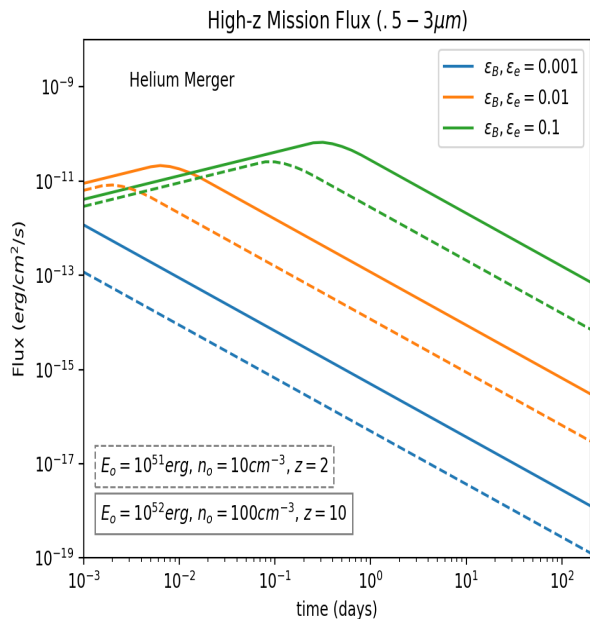


**Fig. 8.** Two fiducial lightcurves in the High-z bandpass for a Helium merger model at a redshift of 10 (solid lines) and 2 (dashed lines) for different values of the fractions of energy in the electrons and magnetic field. The high redshift progenitor has a higher isotropic emitted energy and a higher circumburst density, while the lower redshift progenitor has lower values of each of these quantities.

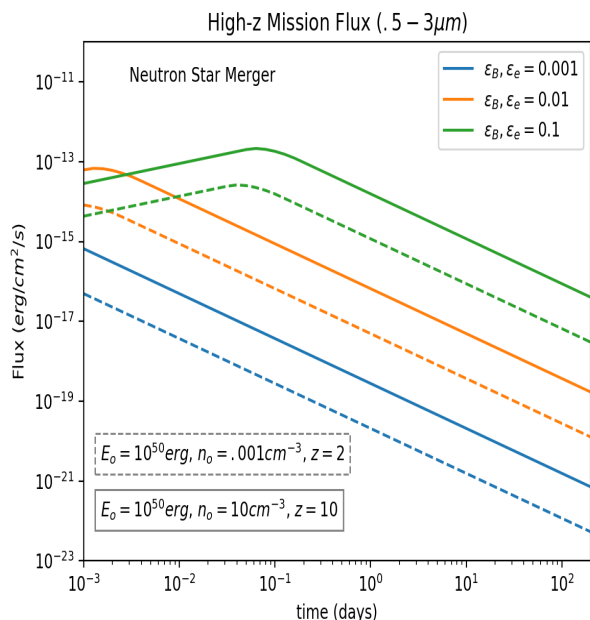


**Fig. 9.** Same as Figure 5, but using fiducial parameters for a Double Neutron Star merger progenitor at a redshift of 10 and 2.

**Table 3.** Variation with Increasing Redshift

Progenitor	Rate	Power	Dur.	CSM
Massive Stars				
Rotating Star	↑	↑?	≡	↓? wind, ↑? ISM
Tidal Locking	↑	↑?	↑?	↓? wind, ↑? ISM
He-He Merger	↑	↑?	↑?	↑ wind, ↑? ISM
He-Merger	↑	↑	≡?	↓ wind, ↑ ISM
Compact Mergers				
NS/NS	≡	↑?	↓?	↑ ISM
NS/BH	↓	↑	↓	↑ ISM
WD/(NS,BH)	↑	?	?	↑ ISM
WD/WD	↓	↑?	↓?	↑ ISM

- **NS/BH mergers:** Although the rate of NS/BH mergers will increase with redshift, larger black hole masses means that fewer of these systems will actually produce disks. Otherwise the trends in properties of this progenitor will follow NS/NS mergers.
- **WD/(NS,BH) mergers:** The rate of these systems will increase with redshift. More massive black holes will produce less powerful bursts but more massive white dwarfs will produce stronger bursts. It is not clear what the final trend will be. Similar effects will alter the duration. The CSM is likely to be higher.
- **WD/WD Mergers:** The flattening of the initial mass function will tend to lower the rate of these mergers, but it is possible that more massive white dwarfs will be produced that both make a GRB fate more likely and produce larger disks that drive more powerful, but shorter, bursts. The CSM is likely to be higher.

Table 3 summarizes the variations in the model with increasing redshift (decreasing metallicity) for the models accretion disk models studied in this paper. At this time, we can, at best, discuss trends and only trends are listed in the table. We show the rate (↑ means an increase with respect to the star formation rate, ≡ means a similar value, and ↓ means an increase with respect to the star formation rate), power (↑, ≡, ↓ mean stronger, equivalent and weaker power respectively), duration (↑, ≡, ↓ correspond to longer, shorter equivalent durations), and the CSM. For the CSM, differences can occur both in the wind and interstellar medium (ISM) properties (↑, ↓ correspond to higher, lower densities).

The trends in power and circumstellar medium will affect the emission from these bursts. Figures 7, 8, and 9 show the expected synchrotron light curves in the High-Z mission bandpass (.5 – 3 μm) for three classes of models: rotating massive star, Helium merger, and NS-NS merger, respectively. For each model, we show light curves at a redshift of 10 (solid lines) and 2 (dashed lines). In addition, we plot the light curves for three different fractions of energy in the magnetic field and electrons (the three different colored lines). Figure 10 shows two sample broadband synchrotron spectra for the two Helium merger models employed in Figure 8, and with the High-Z mission bandpass highlighted.

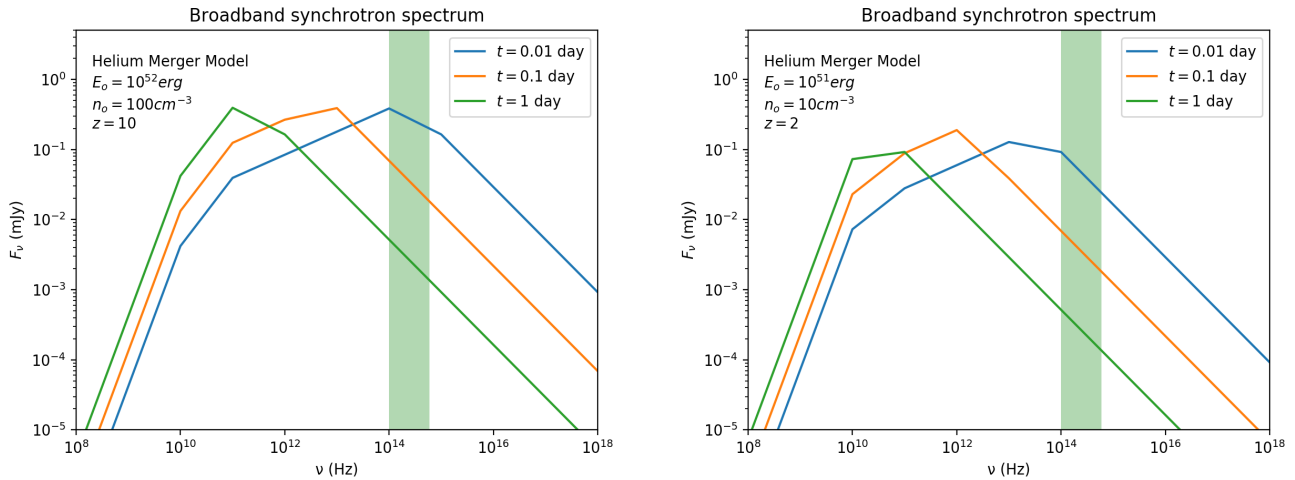


**Fig. 10.** Estimates of the broadband synchrotron spectra for the two Helium merger models shown in Figure 5. The High-Z detector bandpass is highlighted

We note that although one might expect that the high redshift GRBs will exhibit a dimmer light curve due to their distances, the higher presumed emitted energy and circumburst density play against the redshift effect - in some cases the high redshift bursts are expected to have even more flux than low redshift bursts (see, for example, the Helium merger model case in Figure 8). Another way of saying this is that GRBs are not standard candles and their properties at high redshift can make them brighter. Indeed, Lloyd-Ronning et al. [2002] showed - using a large sample of GRBs with psuedo-redshifts - that GRBs exhibit strong luminosity evolution, with higher redshift burst being more luminous.

Broadband observations of high redshift GRBs will potentially allow us to put constraints on the emitted energy and circumburst density, which ultimately, we can tie back to the progenitor itself and thereby learn something about the metallicity and environments of these high redshift systems. Combined with the more detailed, multi-messenger signals of nearby bursts, we can understand the physical mechanisms and underlying physics of GRBs and, in turn, use this understanding of GRBs to probe the early universe.

## Acknowledgements

This work was supported by the US Department of Energy through the Los Alamos National Laboratory. Additional funding was provided by the Laboratory Directed Research and Development Program under project number 20190021DR and the Center for Nonlinear Studies at Los Alamos National Laboratory under project number 20170508DR.

## References

- R. W. Klebesadel, I. B. Strong, and R. A. Olson. Observations of Gamma-Ray Bursts of Cosmic Origin. *ApJL*, 182:L85, June 1973. doi: 10.1086/181225.
- G. J. Fishman, C. A. Meegan, R. B. Wilson, W. S. Paciesas, G. N. Pendleton, B. A. Harmon, J. M. Horack, M. N. Brock, C. Kouveliotou, and M. Finger. Overview of Observations from BATSE on the Compton Observatory. *A&A Sup.*, 97:17, January 1993.
- E. P. Mazets, S. V. Golenetskii, V. N. Ilinskii, V. N. Panov, I. A. Aptekar, I. A. Gurian, I. A. Sokolov, Z. I. Sokolov, and T. V. Kharitonova. *Preliminary results on gamma-ray transients in the Konus experiment on Venera 11 and 12*, pages 124–136. 1983.
- C. Kouveliotou, C. A. Meegan, G. J. Fishman, N. P. Bhat, M. S. Briggs, T. M. Koshut, W. S. Paciesas, and G. N. Pendleton. Identification of two classes of gamma-ray bursts. *ApJL*, 413:L101–L104, August 1993. doi: 10.1086/186969.
- A. J. Levan, N. R. Tanvir, R. L. C. Starling, K. Wiersema, K. L. Page, D. A. Perley, S. Schulze, G. A. Wynn, R. Chornock, J. Hjorth, S. B. Cenko, A. S. Fruchter, P. T. O’Brien, G. C. Brown, R. L. Tunnicliffe, D. Malesani, P. Jakobsson, D. Watson, E. Berger, D. Bersier, B. E. Cobb, S. Covino, A. Cucchiara, A. de Ugarte Postigo, D. B. Fox, A. Gal-Yam, P. Goldoni, J. Gorosabel, L. Kaper, T. Krühler, R. Karjalainen, J. P. Osborne, E. Pian, R. Sánchez-Ramírez, B. Schmidt, I. Skillen, G. Tagliaferri, C. Thöne, O. Vaduvescu, R. A. M. J. Wijers, and B. A. Zauderer. A New Population of Ultra-long Duration Gamma-Ray Bursts. *ApJ*, 781:13, January 2014. doi: 10.1088/0004-637X/781/1/13.
- R. J. Nemiroff. A Century of Gamma Ray Burst Models. *Comments on Astrophysics*, 17:189, 1994.
- M. S. Briggs. Dipole and quadrupole tests of the isotropy of gamma-ray burst locations. *ApJ*, 407:126–134, April



1993. doi: 10.1086/172498.
- E. Costa, F. Frontera, J. Heise, M. Feroci, J. in't Zand, F. Fiore, M. N. Cinti, D. Dal Fiume, L. Nicastro, M. Orlandini, E. Palazzi, M. Rapisarda#, G. Zavattini, R. Jager, A. Parmar, A. Owens, S. Molendi, G. Cusumano, M. C. Maccarone, S. Giarrusso, A. Colletta, L. A. Antonelli, P. Giommi, J. M. Muller, L. Piro, and R. C. Butler. Discovery of an X-ray afterglow associated with the  $\gamma$ -ray burst of 28 February 1997. *Nature*, 387:783–785, June 1997. doi: 10.1038/42885.
- J. van Paradijs, P. J. Groot, T. Galama, C. Kouveliotou, R. G. Strom, J. Telting, R. G. M. Rutten, G. J. Fishman, C. A. Meegan, M. Pettini, N. Tanvir, J. Bloom, H. Pedersen, H. U. Nørregaard-Nielsen, M. Lindenvørnle, J. Melnick, G. Van der Steene, M. Bremer, R. Naber, J. Heise, J. in't Zand, E. Costa, M. Feroci, L. Piro, F. Frontera, G. Zavattini, L. Nicastro, E. Palazzi, K. Bennett, L. Hanlon, and A. Parmar. Transient optical emission from the error box of the  $\gamma$ -ray burst of 28 February 1997. *Nature*, 386:686–689, April 1997. doi: 10.1038/386686a0.
- M. R. Metzger, S. G. Djorgovski, S. R. Kulkarni, C. C. Steidel, K. L. Adelberger, D. A. Frail, E. Costa, and F. Frontera. Spectral constraints on the redshift of the optical counterpart to the  $\gamma$ -ray burst of 8 May 1997. *Nature*, 387:878–880, June 1997. doi: 10.1038/43132.
- D. A. Frail, S. R. Kulkarni, L. Nicastro, M. Feroci, and G. B. Taylor. The radio afterglow from the  $\gamma$ -ray burst of 8 May 1997. *Nature*, 389:261–263, September 1997. doi: 10.1038/38451.
- R. Ramaty, S. Bonazzola, T. L. Cline, D. Kazanas, P. Meszaros, and R. E. Lingenfelter. Origin of the 5 March 1979 gamma-ray transient - A vibrating neutron star. *Nature*, 287:122–124, September 1980. doi: 10.1038/287122a0.
- F. Ma and B. Xie. Super-Giant Glitches and Quark Stars: Sources of Gamma-Ray Bursts? *ApJL*, 462:L63, May 1996. doi: 10.1086/310033.
- R. C. Duncan and C. Thompson. Magnetars. In R. E. Rothschild and R. E. Lingenfelter, editors, *High Velocity Neutron Stars*, volume 366 of *American Institute of Physics Conference Series*, pages 111–117, April 1996. doi: 10.1063/1.50235.
- R. Narayan, B. Paczynski, and T. Piran. Gamma-ray bursts as the death throes of massive binary stars. *ApJL*, 395:L83–L86, August 1992. doi: 10.1086/186493.
- S. E. Woosley. Gamma-ray bursts from stellar mass accretion disks around black holes. *ApJ*, 405:273–277, March 1993. doi: 10.1086/172359.
- C. L. Fryer and S. E. Woosley. Gamma-Ray Bursts from Neutron Star Phase Transitions. *ApJ*, 501:780–786, July 1998a. doi: 10.1086/305866.
- A. Worley, P. G. Krastev, and B.-A. Li. Nuclear Constraints on the Moments of Inertia of Neutron Stars. *ApJ*, 685:390–399, September 2008. doi: 10.1086/589823.
- A. Murguia-Berthier, G. Montes, E. Ramirez-Ruiz, F. De Colle, and W. H. Lee. Necessary Conditions for Short Gamma-Ray Burst Production in Binary Neutron Star Mergers. *ApJL*, 788:L8, June 2014. doi: 10.1088/2041-8205/788/1/L8.
- C. L. Fryer, S. E. Woosley, and D. H. Hartmann. Formation Rates of Black Hole Accretion Disk Gamma-Ray Bursts. *ApJ*, 526:152–177, November 1999a. doi: 10.1086/307992.
- K. Belczynski, J. Klencki, G. Meynet, C. L. Fryer, D. A. Brown, M. Chruslinska, W. Gladysz, R. O’Shaughnessy, T. Bulik, E. Berti, D. E. Holz, D. Gerosa, M. Giersz, S. Ekstrom, C. Georgy, A. Askar, D. Wysocki, and J.-P. Lasota. The origin of low spin of black holes in LIGO/Virgo mergers. *arXiv e-prints*, June 2017.
- A. Heger, S. E. Woosley, and H. C. Spruit. Presupernova Evolution of Differentially Rotating Massive Stars Including Magnetic Fields. *ApJ*, 626:350–363, June 2005. doi: 10.1086/429868.
- B. Paxton, M. Cantiello, P. Arras, L. Bildsten, E. F. Brown, A. Dotter, C. Mankovich, M. H. Montgomery, D. Stello, F. X. Timmes, and R. Townsend. Modules for Experiments in Stellar Astrophysics (MESA): Planets, Oscillations, Rotation, and Massive Stars. *ApJS*, 208:4, September 2013. doi: 10.1088/0067-0049/208/1/4.
- A. I. MacFadyen and S. E. Woosley. Collapsars: Gamma-Ray Bursts and Explosions in “Failed Supernovae”. *ApJ*, 524:262–289, October 1999. doi: 10.1086/307790.
- T. J. Galama, P. M. Vreeswijk, J. van Paradijs, C. Kouveliotou, T. Augusteijn, F. Patat, J. Heise, J. in't Zand, P. J. Groot, R. A. M. J. Wijers, E. Pian, E. Palazzi, F. Frontera, and N. Masetti. On the possible association of SN 1998bw and GRB 980425. *A&A Sup.*, 138:465–466, September 1999. doi: 10.1051/aas:1999311.
- C. L. Fryer, P. A. Mazzali, J. Prochaska, E. Cappellaro, A. Panaitescu, E. Berger, M. van Putten, E. P. J. van den Heuvel, P. Young, A. Hungerford, G. Rockefeller, S.-C. Yoon, P. Podsiadlowski, K. Nomoto, R. Chevalier, B. Schmidt, and S. Kulkarni. Constraints on Type Ib/c Supernovae and Gamma-Ray Burst Progenitors. *PASP*, 119:1211–1232, November 2007. doi: 10.1086/523768.
- H. Sun, B. Zhang, and Z. Li. Extragalactic High-energy Transients: Event Rate Densities and Luminosity Functions. *ApJ*, 812:33, October 2015. doi: 10.1088/0004-637X/812/1/33.
- A. Levan, P. Crowther, R. de Grijs, N. Langer, D. Xu, and S.-C. Yoon. Gamma-Ray Burst Progenitors. *Space Sci. Rev.*, 202:33–78, December 2016. doi: 10.1007/s11214-016-0312-x.
- C. L. Fryer and V. Kalogera. Theoretical Black Hole Mass Distributions. *ApJ*, 554:548–560, June 2001. doi: 10.1086/321359.
- D. Kasen and L. Bildsten. Supernova Light Curves Powered by Young Magnetars. *ApJ*, 717:245–249, July 2010. doi: 10.1088/0004-637X/717/1/245.
- B. D. Metzger, B. Margalit, D. Kasen, and E. Quataert. The diversity of transients from magnetar birth in core collapse supernovae. *MNRAS*, 454:3311–3316, December 2015. doi: 10.1093/mnras/stv2224.
- S.-C. Yoon and N. Langer. On the evolution of rapidly rotating massive white dwarfs towards supernovae or collapses. *A&A*, 435:967–985, June 2005. doi: 10.1051/



- 0004-6361:20042542.
- E. P. J. van den Heuvel and S.-C. Yoon. Long gamma-ray burst progenitors: boundary conditions and binary models. *A&SS*, 311:177–183, October 2007. doi: 10.1007/s10509-007-9583-8.
- C. L. Fryer and A. Heger. Binary Merger Progenitors for Gamma-Ray Bursts and Hypernovae. *ApJ*, 623:302–313, April 2005. doi: 10.1086/428379.
- C. L. Fryer and S. E. Woosley. Helium Star/Black Hole Mergers: A New Gamma-Ray Burst Model. *ApJL*, 502:L9–L12, July 1998b. doi: 10.1086/311493.
- W. Zhang and C. L. Fryer. The Merger of a Helium Star and a Black Hole: Gamma-Ray Bursts. *ApJ*, 550:357–367, March 2001. doi: 10.1086/319734.
- C. Georgy, S. Ekström, A. Granada, G. Meynet, N. Mowlavi, P. Eggenberger, and A. Maeder. Populations of rotating stars. I. Models from 1.7 to 15 M at  $Z = 0.014, 0.006,$  and  $0.002$  with  $\Omega/\Omega_{crit}$  between 0 and 1. *A&A*, 553:A24, May 2013a. doi: 10.1051/0004-6361/201220558.
- D. Gagnier, M. Rieutord, C. Charbonnel, B. Putigny, and F. Espinosa Lara. Evolution of rotation in rapidly rotating early-type stars during the main sequence with 2D models. *arXiv e-prints*, April 2019.
- L. H. Frey, C. L. Fryer, and P. A. Young. Can Stellar Mixing Explain the Lack of Type Ib Supernovae in Long-duration Gamma-Ray Bursts? *ApJL*, 773:L7, August 2013. doi: 10.1088/2041-8205/773/1/L7.
- M. Livio and P. Mazzali. On the progenitors of Type Ia supernovae. *Phys. Rep.*, 736:1–23, March 2018. doi: 10.1016/j.physrep.2018.02.002.
- C. Fryer, W. Benz, M. Herant, and S. A. Colgate. What Can the Accretion-induced Collapse of White Dwarfs Really Explain? *ApJ*, 516:892–899, May 1999b. doi: 10.1086/307119.
- C. L. Fryer, P. J. Brown, F. Bufano, J. A. Dahl, C. J. Fontes, L. H. Frey, S. T. Holland, A. L. Hungerford, S. Immler, P. Mazzali, P. A. Milne, E. Scannapieco, N. Weinberg, and P. A. Young. Spectra and Light Curves of Failed Supernovae. *ApJ*, 707:193–207, December 2009. doi: 10.1088/0004-637X/707/1/193.
- J. Schwab. *The Long-Term Outcomes of Double White Dwarf Mergers*. PhD thesis, University of California, Berkeley, 2016.
- C. L. Fryer, S. E. Woosley, M. Herant, and M. B. Davies. Merging White Dwarf/Black Hole Binaries and Gamma-Ray Bursts. *ApJ*, 520:650–660, August 1999c. doi: 10.1086/307467.
- B. D. Metzger and E. Berger. What is the Most Promising Electromagnetic Counterpart of a Neutron Star Binary Merger? *ApJ*, 746:48, February 2012. doi: 10.1088/0004-637X/746/1/48.
- M. Ruffert and H.-T. Janka. Merging Neutron Stars. In R. E. Schielicke, editor, *Reviews in Modern Astronomy*, volume 10 of *Reviews in Modern Astronomy*, pages 201–218, 1997.
- S. Rosswog and E. Ramirez-Ruiz. Dynamos, Superpulsars and Gamma-ray Bursts. In E. Fenimore and M. Galassi, editors, *Gamma-Ray Bursts: 30 Years of Discovery*, volume 727 of *American Institute of Physics Conference Series*, pages 361–365, September 2004. doi: 10.1063/1.1810865.
- S. Rosswog. Fallback accretion in the aftermath of a compact binary merger. *MNRAS*, 376:L48–L51, March 2007. doi: 10.1111/j.1745-3933.2007.00284.x.
- C. L. Fryer, K. Belczynski, E. Ramirez-Ruiz, S. Rosswog, G. Shen, and A. W. Steiner. The Fate of the Compact Remnant in Neutron Star Mergers. *ApJ*, 812:24, October 2015. doi: 10.1088/0004-637X/812/1/24.
- R. Popham, S. E. Woosley, and C. Fryer. Hyperaccreting Black Holes and Gamma-Ray Bursts. *ApJ*, 518:356–374, June 1999. doi: 10.1086/307259.
- H.-T. Janka, T. Eberl, M. Ruffert, and C. L. Fryer. Black Hole-Neutron Star Mergers as Central Engines of Gamma-Ray Bursts. *ApJL*, 527:L39–L42, December 1999. doi: 10.1086/312397.
- M. Ruffert, H.-T. Janka, and T. Eberl. Neutron star-black hole mergers. *Nuclear Physics B Proceedings Supplements*, 80:06, January 2000.
- M. Shibata and K. Uryu. Merger of black hole neutron star binaries in full general relativity. *Classical and Quantum Gravity*, 24:S125–S137, June 2007. doi: 10.1088/0264-9381/24/12/S09.
- K. Belczynski, R. E. Taam, E. Rantsiou, and M. van der Sluys. Black Hole Spin Evolution: Implications for Short-Hard Gamma-Ray Bursts and Gravitational Wave Detection. *ApJ*, 682:474–486, July 2008. doi: 10.1086/589609.
- I. Contopoulos and A. Spitkovsky. Revised Pulsar Spindown. *ApJ*, 643:1139–1145, June 2006. doi: 10.1086/501161.
- W. Fong, B. D. Metzger, E. Berger, and F. Özel. Radio Constraints on Long-lived Magnetar Remnants in Short Gamma-Ray Bursts. *ApJ*, 831:141, November 2016. doi: 10.3847/0004-637X/831/2/141.
- L. Piro, E. Troja, B. Zhang, G. Ryan, H. van Eerten, R. Ricci, M. H. Wieringa, A. Tiengo, N. R. Butler, S. B. Cenko, O. D. Fox, H. G. Khandrika, G. Novara, A. Rossi, and T. Sakamoto. A long-lived neutron star merger remnant in GW170817: constraints and clues from X-ray observations. *MNRAS*, 483:1912–1921, February 2019. doi: 10.1093/mnras/sty3047.
- J. S. Bloom, S. Sigurdsson, and O. R. Pols. The spatial distribution of coalescing neutron star binaries: implications for gamma-ray bursts. *MNRAS*, 305:763–769, May 1999. doi: 10.1046/j.1365-8711.1999.02437.x.
- P. M. Vreeswijk, A. Fruchter, L. Kaper, E. Rol, T. J. Galama, J. van Paradijs, C. Kouveliotou, R. A. M. J. Wijers, E. Pian, E. Palazzi, N. Masetti, F. Frontera, S. Savaglio, K. Reinsch, F. V. Hessman, K. Beuermann, H. Nicklas, and E. P. J. van den Heuvel. VLT Spectroscopy of GRB 990510 and GRB 990712: Probing the Faint and Bright Ends of the Gamma-Ray Burst Host Galaxy Population. *ApJ*, 546:672–680, January 2001. doi: 10.1086/318308.
- J. S. Bloom. Toward an Understanding of the Progenitors of Gamma-Ray Bursts. *PASP*, 115:271–271, February 2003. doi: 10.1086/345917.

- A. S. Fruchter, A. J. Levan, L. Strolger, P. M. Vreeswijk, S. E. Thorsett, D. Bersier, I. Burud, J. M. Castro Cerón, A. J. Castro-Tirado, C. Conselice, T. Dahlen, H. C. Ferguson, J. P. U. Fynbo, P. M. Garnavich, R. A. Gibbons, J. Gorosabel, T. R. Gull, J. Hjorth, S. T. Holland, C. Kouveliotou, Z. Levay, M. Livio, M. R. Metzger, P. E. Nugent, L. Petro, E. Pian, J. E. Rhoads, A. G. Riess, K. C. Sahu, A. Smette, N. R. Tanvir, R. A. M. J. Wijers, and S. E. Woosley. Long  $\gamma$ -ray bursts and core-collapse supernovae have different environments. *Nature*, 441: 463–468, May 2006. doi: 10.1038/nature04787.
- W. Fong, E. Berger, R. Chornock, R. Margutti, A. J. Levan, N. R. Tanvir, R. L. Tunnicliffe, I. Czekala, D. B. Fox, D. A. Perley, S. B. Cenko, B. A. Zauderer, T. Laskar, S. E. Persson, A. J. Monson, D. D. Kelson, C. Birk, D. Murphy, M. Servillat, and G. Anglada. Demographics of the Galaxies Hosting Short-duration Gamma-Ray Bursts. *ApJ*, 769:56, May 2013. doi: 10.1088/0004-637X/769/1/56.
- W. Fong and E. Berger. The Locations of Short Gamma-Ray Bursts as Evidence for Compact Object Binary Progenitors. *ApJ*, 776:18, October 2013. doi: 10.1088/0004-637X/776/1/18.
- B. P. Abbott, R. Abbott, T. D. Abbott, F. Acernese, K. Ackley, C. Adams, T. Adams, P. Addesso, R. X. Adhikari, V. B. Adya, and et al. Gravitational Waves and Gamma-Rays from a Binary Neutron Star Merger: GW170817 and GRB 170817A. *ApJL*, 848:L13, October 2017. doi: 10.3847/2041-8213/aa920c.
- V. Savchenko, C. Ferrigno, E. Kuulkers, A. Bazzano, E. Bozzo, S. Brandt, J. Chenevez, T. J.-L. Courvoisier, R. Diehl, A. Domingo, L. Hanlon, E. Jourdain, A. von Kienlin, P. Laurent, F. Lebrun, A. Lutovinov, A. Martin-Carrillo, S. Mereghetti, L. Natalucci, J. Rodi, J.-P. Roques, R. Sunyaev, and P. Ubertini. INTEGRAL Detection of the First Prompt Gamma-Ray Signal Coincident with the Gravitational-wave Event GW170817. *ApJL*, 848:L15, October 2017. doi: 10.3847/2041-8213/aa8f94.
- E. Troja, L. Piro, H. van Eerten, R. T. Wollaeger, M. Im, O. D. Fox, N. R. Butler, S. B. Cenko, T. Sakamoto, C. L. Fryer, R. Ricci, A. Lien, R. E. Ryan, O. Korobkin, S.-K. Lee, J. M. Burgess, W. H. Lee, A. M. Watson, C. Choi, S. Covino, P. D’Avanzo, C. J. Fontes, J. B. González, H. G. Khandrika, J. Kim, S.-L. Kim, C.-U. Lee, H. M. Lee, A. Kutayev, G. Lim, R. Sánchez-Ramírez, S. Veilleux, M. H. Wieringa, and Y. Yoon. The X-ray counterpart to the gravitational-wave event GW170817. *Nature*, 551:71–74, November 2017. doi: 10.1038/nature24290.
- K. P. Mooley, D. A. Frail, D. Dobie, E. Lenc, A. Corsi, K. De, A. J. Nayana, S. Makhathini, I. Heywood, T. Murphy, D. L. Kaplan, P. Chandra, O. Smirnov, E. Nakar, G. Hallinan, F. Camilo, R. Fender, S. Goedhart, P. Groot, M. M. Kasliwal, S. R. Kulkarni, and P. A. Woudt. A Strong Jet Signature in the Late-time Light Curve of GW170817. *ApJL*, 868:L11, November 2018. doi: 10.3847/2041-8213/aaeda7.
- J. M. Lattimer and D. N. Schramm. Black-hole-neutron-star collisions. *ApJL*, 192:L145–L147, September 1974. doi: 10.1086/181612.
- E. Berger, W. Fong, and R. Chornock. An r-process Kilonova Associated with the Short-hard GRB 130603B. *ApJL*, 774:L23, September 2013. doi: 10.1088/2041-8205/774/2/L23.
- N. R. Tanvir, A. J. Levan, A. S. Fruchter, J. Hjorth, R. A. Hounsell, K. Wiersema, and R. L. Tunnicliffe. A ‘kilonova’ associated with the short-duration  $\gamma$ -ray burst GRB 130603B. *Nature*, 500:547–549, August 2013. doi: 10.1038/nature12505.
- M. M. Kasliwal, O. Korobkin, R. M. Lau, R. Wollaeger, and C. L. Fryer. Infrared Emission from Kilonovae: The Case of the Nearby Short Hard Burst GRB 160821B. *ApJL*, 843:L34, July 2017. doi: 10.3847/2041-8213/aa799d.
- C. Freiburghaus, S. Rosswog, and F.-K. Thielemann. R-Process in Neutron Star Mergers. *ApJL*, 525:L121–L124, November 1999. doi: 10.1086/312343.
- S. Goriely, A. Bauswein, and H.-T. Janka. r-process Nucleosynthesis in Dynamically Ejected Matter of Neutron Star Mergers. *ApJL*, 738:L32, September 2011. doi: 10.1088/2041-8205/738/2/L32.
- L. F. Roberts, D. Kasen, W. H. Lee, and E. Ramirez-Ruiz. Electromagnetic Transients Powered by Nuclear Decay in the Tidal Tails of Coalescing Compact Binaries. *ApJL*, 736:L21, July 2011. doi: 10.1088/2041-8205/736/1/L21.
- O. Korobkin, S. Rosswog, A. Arcones, and C. Winteler. On the astrophysical robustness of the neutron star merger r-process. *MNRAS*, 426:1940–1949, November 2012. doi: 10.1111/j.1365-2966.2012.21859.x.
- S. Richers, D. Kasen, E. O’Connor, R. Fernandez, and C. D. Ott. Monte carlo neutrino transport through remnant disks from neutron star mergers. *The Astrophysical Journal*, 813(1):38, 2015. URL <http://stacks.iop.org/0004-637X/813/i=1/a=38>.
- G. Montes, E. Ramirez-Ruiz, J. Naiman, S. Shen, and W. H. Lee. Transport and Mixing of r-process Elements in Neutron Star Binary Merger Blast Waves. *ApJ*, 830: 12, October 2016. doi: 10.3847/0004-637X/830/1/12.
- Y. Sekiguchi, K. Kiuchi, K. Kyutoku, M. Shibata, and K. Taniguchi. Dynamical mass ejection from the merger of asymmetric binary neutron stars: Radiation-hydrodynamics study in general relativity. *PRD*, 93(12): 124046, June 2016. doi: 10.1103/PhysRevD.93.124046.
- D. Radice, F. Galeazzi, J. Lippuner, L. F. Roberts, C. D. Ott, and L. Rezzolla. Dynamical mass ejection from binary neutron star mergers. *MNRAS*, 460:3255–3271, August 2016. doi: 10.1093/mnras/stw1227.
- M. Shibata, K. Kiuchi, and Y.-i. Sekiguchi. General relativistic viscous hydrodynamics of differentially rotating neutron stars. *PRD*, 95(8):083005, April 2017. doi: 10.1103/PhysRevD.95.083005.
- L. Bovard, D. Martin, F. Guercilena, A. Arcones, L. Rezzolla, and O. Korobkin. r-process nucleosynthesis from matter ejected in binary neutron star mergers. *PRD*, 96(12):124005, December 2017. doi: 10.1103/PhysRevD.

- 96.124005.
- Francois Foucart. Monte carlo closure for moment-based transport schemes in general relativistic radiation hydrodynamic simulations. *Monthly Notices of the Royal Astronomical Society*, 475(3):4186–4207, 2018. doi: 10.1093/mnras/sty108. URL <http://dx.doi.org/10.1093/mnras/sty108>.
- C. L. Fryer. Neutrinos from fallback onto newly formed neutron stars. *ApJ*, 699:409–420, July 2009. doi: 10.1088/0004-637X/699/1/409.
- J. Lippuner and L. F. Roberts. r-process Lanthanide Production and Heating Rates in Kilonovae. *ApJ*, 815:82, December 2015. doi: 10.1088/0004-637X/815/2/82.
- G. Magkotsios, F. X. Timmes, A. L. Hungerford, C. L. Fryer, P. A. Young, and M. Wiescher. Trends in  $^{44}\text{Ti}$  and  $^{56}\text{Ni}$  from core-collapse supernovae. *ApJS*, 191:66–95, November 2010. doi: 10.1088/0067-0049/191/1/66.
- Francois Foucart et al. Post-merger evolution of a neutron star-black hole binary with neutrino transport. *Phys. Rev. D*, 91:124021, Jun 2015. doi: 10.1103/PhysRevD.91.124021. URL <https://link.aps.org/doi/10.1103/PhysRevD.91.124021>.
- Fatemeh Hossein Nouri, Matthew D. Duez, Francois Foucart, M. Brett Deaton, Roland Haas, Milad Haddadi, Lawrence E. Kidder, Christian D. Ott, Harald P. Pfeiffer, Mark A. Scheel, and Bela Szilagyi. Evolution of the magnetized, neutrino-cooled accretion disk in the aftermath of a black hole-neutron star binary merger. *Phys. Rev. D*, 97:083014, Apr 2018. doi: 10.1103/PhysRevD.97.083014. URL <https://link.aps.org/doi/10.1103/PhysRevD.97.083014>.
- D. M. Siegel and B. D. Metzger. Three-dimensional grmhd simulations of neutrino-cooled accretion disks from neutron star mergers. *The Astrophysical Journal*, 858(1):52, 2018. URL <http://stacks.iop.org/0004-637X/858/i=1/a=52>.
- R. Fernández et al. Long-term GRMHD Simulations of Neutron Star Merger Accretion Disks: Implications for Electromagnetic Counterparts. *ArXiv e-prints*, August 2018.
- J. M. Miller, B. R. Ryan, and J. C. Dolence.  $\nu$  bh-light: Radiation GRMHD for Neutrino-driven Accretion Flows. *ApJS*, 241:30, April 2019. doi: 10.3847/1538-4365/ab09fc.
- B. D. Metzger and R. Fernández. Red or blue? A potential kilonova imprint of the delay until black hole formation following a neutron star merger. *MNRAS*, 441:3444–3453, July 2014. doi: 10.1093/mnras/stu802.
- B. Côté, C. L. Fryer, K. Belczynski, O. Korobkin, M. Chruslińska, N. Vassh, M. R. Mumpower, J. Lippuner, T. M. Sprouse, R. Surman, and R. Wollaeger. The Origin of r-process Elements in the Milky Way. *ApJ*, 855:99, March 2018a. doi: 10.3847/1538-4357/aaad67.
- R. T. Wollaeger, O. Korobkin, C. J. Fontes, S. K. Rosswog, W. P. Even, C. L. Fryer, J. Sollerman, A. L. Hungerford, D. R. van Rossum, and A. B. Wollaber. Impact of ejecta morphology and composition on the electromagnetic signatures of neutron star mergers. *MNRAS*, 478:3298–3334, August 2018. doi: 10.1093/mnras/sty1018.
- B. Côté, K. Belczynski, C. L. Fryer, C. Ritter, A. Paul, B. Wehmeyer, and B. W. O’Shea. Advanced LIGO Constraints on Neutron Star Mergers and r-process Sites. *ApJ*, 836:230, February 2017. doi: 10.3847/1538-4357/aa5c8d.
- V. Kalogera, C. Kim, D. R. Lorimer, M. Burgay, N. D’Amico, A. Possenti, R. N. Manchester, A. G. Lyne, B. C. Joshi, M. A. McLaughlin, M. Kramer, J. M. Sarkissian, and F. Camilo. The Cosmic Coalescence Rates for Double Neutron Star Binaries. *ApJL*, 601:L179–L182, February 2004. doi: 10.1086/382155.
- H.-Y. Chen and D. E. Holz. Gamma-Ray-Burst Beaming and Gravitational-Wave Observations. *Physical Review Letters*, 111(18):181101, November 2013. doi: 10.1103/PhysRevLett.111.181101.
- M. Dominik, K. Belczynski, C. Fryer, D. E. Holz, E. Berti, T. Bulik, I. Mandel, and R. O’Shaughnessy. Double Compact Objects. I. The Significance of the Common Envelope on Merger Rates. *ApJ*, 759:52, November 2012. doi: 10.1088/0004-637X/759/1/52.
- B. Côté, M. Eichler, A. Arcones, C. J. Hansen, P. Simonetti, A. Frebel, C. L. Fryer, M. Pignatari, M. Reichert, K. Belczynski, and F. Matteucci. Neutron Star Mergers Might not be the Only Source of r-Process Elements in the Milky Way. *arXiv e-prints*, September 2018b.
- A. Rossi, G. Stratta, E. Maiorano, D. Spighi, N. Masetti, E. Palazzi, A. Gardini, A. Melandri, L. Nicastro, E. Pian, M. Branchesi, M. Dadina, V. Testa, S. Brocato, S. Benetti, R. Ciolfi, S. Covino, V. D’Elia, A. Grado, L. Izzo, A. Perego, S. Piranomonte, R. Salvaterra, J. Selsing, L. Tomasella, S. Yang, and D. Vergani. A comparison between short GRB afterglows and KN170817: shedding light on kilonovae properties. *arXiv e-prints*, January 2019.
- Y. Zhu, R. T. Wollaeger, N. Vassh, R. Surman, T. M. Sprouse, M. R. Mumpower, P. Möller, G. C. McLaughlin, O. Korobkin, T. Kawano, P. J. Jaffke, E. M. Holmbeck, C. L. Fryer, W. P. Even, A. J. Couture, and J. Barnes. Californium-254 and Kilonova Light Curves. *ApJL*, 863:L23, August 2018. doi: 10.3847/2041-8213/aad5de.
- C. L. Fryer and K. C. B. New. Gravitational Waves from Gravitational Collapse. *Living Reviews in Relativity*, 14:1, January 2011. doi: 10.12942/lrr-2011-1.
- C. L. Fryer, D. E. Holz, and S. A. Hughes. Gravitational Wave Emission from Core Collapse of Massive Stars. *ApJ*, 565:430–446, January 2002. doi: 10.1086/324034.
- K. Belczynski, D. E. Holz, C. L. Fryer, E. Berger, D. H. Hartmann, and B. O’Shea. On the Origin of the Highest Redshift Gamma-Ray Bursts. *ApJ*, 708:117–126, January 2010. doi: 10.1088/0004-637X/708/1/117.
- J.-C. Passy, O. De Marco, C. L. Fryer, F. Herwig, S. Diehl, J. S. Oishi, M.-M. Mac Low, G. L. Bryan, and G. Rockefeller. Simulating the Common Envelope Phase of a Red Giant Using Smoothed-particle Hydrodynamics and Uniform-grid Codes. *ApJ*, 744:52, January 2012. doi: 10.1088/0004-637X/744/1/52.

- N. M. Lloyd-Ronning, C. L. Fryer, and E. Ramirez-Ruiz. Cosmological Aspects of Gamma-Ray Bursts: Luminosity Evolution and an Estimate of the Star Formation Rate at High Redshifts. *ApJ*, 574:554–565, August 2002. doi: 10.1086/341059.
- A. Pescalli, G. Ghirlanda, R. Salvaterra, G. Ghisellini, S. D. Vergani, F. Nappo, O. S. Salafia, A. Melandri, S. Covino, and D. Götz. The rate and luminosity function of long gamma ray bursts. *A&A*, 587:A40, March 2016. doi: 10.1051/0004-6361/201526760.
- P. A. Young and C. L. Fryer. The Local Environments of Long-Duration Gamma-Ray Bursts. *ApJ*, 670:584–591, November 2007. doi: 10.1086/521695.
- M. Dominik, K. Belczynski, C. Fryer, D. E. Holz, E. Berti, T. Bulik, I. Mandel, and R. O’Shaughnessy. Double Compact Objects. II. Cosmological Merger Rates. *ApJ*, 779:72, December 2013. doi: 10.1088/0004-637X/779/1/72.
- S. Ekström, C. Georgy, P. Eggenberger, G. Meynet, N. Mowlavi, A. Wyttenbach, A. Granada, T. Decressin, R. Hirschi, U. Frischknecht, C. Charbonnel, and A. Maeder. Grids of stellar models with rotation. I. Models from 0.8 to 120 M at solar metallicity ( $Z = 0.014$ ). *A&A*, 537:A146, January 2012. doi: 10.1051/0004-6361/201117751.
- C. Georgy, S. Ekström, G. Meynet, P. Massey, E. M. Levesque, R. Hirschi, P. Eggenberger, and A. Maeder. Grids of stellar models with rotation. II. WR populations and supernovae/GRB progenitors at  $Z = 0.014$ . *A&A*, 542:A29, June 2012. doi: 10.1051/0004-6361/201118340.
- C. Georgy, S. Ekström, P. Eggenberger, G. Meynet, L. Haemmerlé, A. Maeder, A. Granada, J. H. Groh, R. Hirschi, N. Mowlavi, N. Yusof, C. Charbonnel, T. Decressin, and F. Barblan. Grids of stellar models with rotation. III. Models from 0.8 to 120 M at a metallicity  $Z = 0.002$ . *A&A*, 558:A103, October 2013b. doi: 10.1051/0004-6361/201322178.
- S. E. Woosley, A. Heger, and T. A. Weaver. The evolution and explosion of massive stars. *Reviews of Modern Physics*, 74:1015–1071, November 2002. doi: 10.1103/RevModPhys.74.1015.
- B. K. Wiggins, C. L. Fryer, J. M. Smidt, D. Hartmann, N. Lloyd-Ronning, and C. Belczynski. The Location and Environments of Neutron Star Mergers in an Evolving Universe. *ApJ*, 865:27, September 2018. doi: 10.3847/1538-4357/aad2d4.